von Keyserlingk, J., de Hoop, M., Mayor, A. G., Dekker, S. C., Rietkerk, M., Förster, S. (2021): Resilience of vegetation to drought: Studying the effect of grazing in a Mediterranean rangeland using satellite time series. - Remote Sensing of Environment, 255, 112270.

https://doi.org/10.1016/j.rse.2020.112270

Resilience of vegetation to drought: studying the effect of grazing in a Mediterranean rangeland using satellite time series

Authors:

J. von Keyserlingk*[1,2,3] & M. de Hoop*[4,] A.G. Mayor[4], S.C. Dekker[4], M. Rietkerk[4], S. Foerster[3]

*authors contributed equally

[1]University of Potsdam, Institute of Environmental Sciences and Geography, Karl-Liebknecht-Str. 24-25, D-14476 Potsdam, Germany

[2]TU Berlin, Ecohydrology and Landscape Evaluation, Institute of Ecology, Ernst-Reuter-Platz 1, D-10587 Berlin, Germany

[3]GFZ German Research Centre for Geosciences, Section Remote Sensing and Geoinformatics, Telegrafenberg, D-14473 Potsdam, Germany

[4]Utrecht University, Environmental Sciences, Copernicus Institute of Sustainable Development, Postbus 80.115, 3508TC Utrecht, The Netherlands

Email Addresses: j.keyserlingk@outlook.de, m.dehoop@outlook.com

Corresponding author: Jennifer von Keyserlingk

Abstract

Understanding how resilient rangelands are to climatic disturbances such as drought is of major importance to land managers. The resilience of ecosystems can be reduced by livestock grazing and by environmental conditions. Most studies quantifying resilience are based on model simulations. However, natural time series from satellite data offer the possibility to infer aspects of resilience from real systems. The objective of this study was to investigate two aspects of ecological resilience, namely resistance to climate variability and recovery from drought, by applying a change detection method (Breaks For Additive Seasonal and Trend; BFAST) spatially on a 28-year Landsat NDVI time series in a dry rangeland in southern Cyprus. First, we used the number of breakpoints fitted by the BFAST model as an inverted proxy for long-term vegetation resistance to climate variability (the ability to withstand change during a disturbance reduces the likelihood to trigger a breakpoint in the time series). Second, we used the linear slope of the BFAST model after a known drought as a proxy of the recovery rate of the vegetation. This information was then used to analyse the spatial distribution of the total number of breakpoints and of the NDVI recovery trend in relation to grazing and environmental properties. Our results show that high NDVI and a northern orientation (i.e. favourable environmental conditions) were associated with a highly resilient system, due to high resistance to climate variability and fast recovery after drought. Intermediate conditions were associated with low resistance. Unfavourable conditions and high grazing intensities were associated with an unresponsive ecosystem state characterised by high resistance and slow recovery after a drought event. Low grazing intensities positively affected the NDVI recovery trend, but did not improve resistance. On northern slopes, terrain slope had a positive effect on the NDVI recovery trend, while on southern slopes it had a negative effect. Our satellite-driven approach has a strong potential for resilience monitoring, because it can be applied on broad spatial and temporal scales in areas with low availability of field data. Moreover, it allows to jointly extract two important components of resilience: resistance and recovery rate.

Author Keywords: Landsat, time series, change detection, resilience, resistance, recovery, grazing, drought

1. Introduction

In southern Europe, rangelands are strained by an erratic Mediterranean climate with frequent droughts and intensive land use practices, such as livestock grazing. This combination of anthropogenic and climatic stressors makes them particularly susceptible to land degradation. In the last decades, there has been an increase in temperature throughout Europe as well as decreasing precipitation in southern Europe (IPCC, 2014). A marked increase in extreme climate events, such as heavy precipitation events and droughts is predicted for Europe due to climate change, (IPCC, 2014). How resilient rangelands are to climatic anomalies and how this is affected by land use, is therefore of major importance to land managers. We developed an innovative satellite-driven approach to spatially quantify two aspects of ecological resilience: (i) resistance to climate variability and (ii) recovery from drought, with different pressures due to grazing.

Ecological resilience has been described by Holling (1996, 1973) as a system's ability to absorb perturbations and persist without being flipped into another regime of behaviour, also termed "basin of attraction". In resilience theory, this concept has often been characterised by use of a "ball-in-a-cup" model (see e.g. Fig. 2 in Scheffer et al., 2012 for a graphical representation), where valleys represent basins of attraction and the ball represents the system state (Dakos et al., 2014; Holling, 1973; Peterson et al., 1998; Scheffer et al., 2001, 2012, 2015; van Nes and Scheffer, 2007). In this picture, resilience is theoretically depicted as the size of the basins of attraction. However, ecological resilience is hard to measure directly (van Nes and Scheffer, 2007). As a good proxy for the size of the basin of attraction the rate of recovery after small perturbations has been proposed (Scheffer et al., 2015; van Nes and Scheffer, 2007). The recovery rate becomes slower when ecological resilience is reduced. This relationship has been shown to hold true also for larger experimental or natural perturbations (van de Leemput et al., 2018; van Nes and Scheffer, 2007). In this work, we use the recovery rate of vegetation after a drought to approximate the ecological resilience of the system to drought. To complement recovery rate as a measure of resilience, we additionally assess the long-term

resistance of the ecosystem to climate variability over 28 years. This was motivated by recent studies that emphasize the need to jointly consider recovery and resistance when measuring the resilience of ecosystems to disturbance (Hodgson et al., 2015; Ingrisch and Bahn, 2018; Nimmo et al., 2015). We base our measure of resistance on Hodgson et al. (2015), where resistance is described as the "instantaneous impact of exogenous disturbances on the system state". In our study, we consider climate variability as an external process affecting vegetation dynamics.

Most studies attempting a quantification of ecological resilience have been based on simulated data. Yet, with the increasing availability of remotely sensed data, satellite-driven approaches have been established (see e.g. Washington-Allen et al., 2008; Frazier et al., 2013; De Keersmaecker et al., 2015; Schwalm et al., 2017). In this study, we used remotely sensed time series of the Normalized Difference Vegetation Index (NDVI), which provide an excellent basis to study long-term vegetation dynamics as well as vegetation responses to disturbances such as drought. Satellite data has the advantage of being consistently collected over time at a global scale. This consistency in measurement makes it possible to monitor vegetation dynamics at a high cadence, instead of reverting to temporal snapshots, e.g. before and after a disturbance. According to Kennedy et al. (2014) a temporal consistency of observation is critical for understanding ecosystem dynamics. The Landsat archive contains the longest record of global- scale medium spatial resolution earth observation data (Hansen and Loveland, 2012). The Landsat 5 TM, 7 ETM+ and 8 OLI sensors have a repeat cycle of 16 days each, while satellite orbits are offset to allow 8-day repeat coverage of any Landsat scene when two Landsat sensors are flying concurrently. Landsat TM, ETM+ and OLI data are collected at a spatial resolution of 30 m in the VIS, NIR and SWIR spectral bands. Its spatial scale makes Landsat data especially suitable for addressing ecological questions (Kennedy et al., 2014) and allows for the detection of small changes (Zhu and Woodcock, 2014). However, its relatively low temporal frequency is a drawback, especially since the number of pixels available for the analysis of vegetation dynamics is reduced by cloud coverage. Furthermore, there is large variation in the regional annual coverage of Landsat 5 data due to technical problems with downlinking acquired data to the ground stations (Goward et al., 2006). In most places

of the world outside the United States this large variation yields a far lower frequency of available images, with several long data gaps, especially in the 80s and 90s. After the launch of Landsat 7 ETM+ in 1999 the number of acquisitions increased with the introduction of a global acquisition plan. Accordingly, some international ground stations switched their reception from Landsat 5 TM to Landsat 7 ETM+. However, several of them changed their operations again to Landsat 5 TM after the failure of the Landsat 7 ETM+ scan line corrector system in May 2003 (Kovalskyy and Roy, 2013).

The NDVI is a measure of the photosynthetic activity of plants. Since the earliest reported use of the NDVI in the Great Plains study by Rouse et al. (1973) it has already been widely applied to study vegetation dynamics, monitor habitat degradation, as well as effects of disturbances such as drought (Pettorelli et al., 2005). While the NDVI is known to be affected by soil background, Weiss et al. (2004) demonstrated its effectiveness for capturing the intra- and inter-annual variation in dryland vegetation. Gaitán et al. (2013) found the NDVI to be the best predictor of ecosystem attributes, such as vegetation cover, compared to several other vegetation indices in a dryland. Furthermore, NDVI variability was shown to agree with precipitation variability (Gaitán et al., 2013; Helman et al., 2014), and to correlate with drought in large areas of the world (Vicente-Serrano et al., 2013). Therefore, in this study we use the NDVI as a well-established vegetation index to assess the response of vegetation to climate variability.

Satellite time series offer the possibility to infer aspects of resilience from real world systems. Van Nes and Scheffer (2007) suggest estimating recovery rates after stochastic disturbances in natural time series as an alternative to experimental perturbations. However, especially in seasonal, climate-driven time series of vegetation with large natural variation, it is difficult to distinguish between the intrinsic seasonal variation and a disturbance (e.g. see extensive review on change in grasslands in Henebry, 2019). To this effect, several change detection methods have been developed, which are able to detect abrupt changes (henceforth “breakpoints”) in time series, while accounting for seasonality and trends present in the data (Ben Abbes et al., 2018). One of these is the Breaks For Additive Seasonal and Trend

(BFAST) method (Verbesselt et al., 2012, 2010a, 2010b). BFAST type approaches have been validated and tested for detecting and monitoring abrupt vegetation changes in forested landscape (DeVries et al., 2015b; Dutrieux et al., 2015; Lambert et al., 2013; Verbesselt et al., 2012, 2010a), as well as in drylands (Browning et al., 2017; Watts and Laffan, 2014), and were found successful in detecting drought induced trend changes (Huang et al., 2014; Verbesselt et al., 2012). Even though the original BFAST method was developed for regularly spaced time series, adapted versions of the algorithm that are able to deal with missing data have been applied in several studies (de Jong et al., 2013; DeVries et al., 2016; Verbesselt et al., 2012). In this study, we applied an adapted version of BFAST, based on DeVries et al. (2016), to a dense long-term Landsat time series of the NDVI, making use of all available data.

Intensive livestock grazing has been shown to reduce the resilience of dryland ecosystems (Holling, 1996; Ruppert et al., 2015). For example, rangelands in savannas of southern Africa used for cattle grazing lose species diversity in favour of grazing resistant species, which are often less resilient to drought; this loss in diversity increases the likelihood for the system to flip into another system state dominated by woody shrubs (Dougill et al., 1999; Holling, 1996). Overgrazing reduces vegetation cover (Kawamura et al., 2005) and trampling further damages the soil, which strongly enhances the ecosystems susceptibility to soil erosion (Zhou et al., 2010). Southern-oriented slopes (in the northern hemisphere), as well as steep slopes, are particularly vulnerable to soil erosion processes. A southern orientation means a maximum exposure to solar radiation, which leads to particularly high evapotranspiration rates. On steep slopes, the time for water infiltration into the soil is low, yielding high water runoff rates. In both cases, the conditions are unfavourable for vegetation. The combined effect of a loss of vegetation cover and soil erosion reduces the capacity of the ecosystem to resist and recover from drought (Mayor et al., 2013; Zhou et al., 2010).

In this study, we aimed to investigate two aspects of ecological resilience: (i) resistance to climate variability and (ii) recovery from drought by applying a change detection method (BFAST) spatially on

a 28-year Landsat NDVI time series in a dry rangeland in southern Cyprus. As a relative inverted measure of ecosystem resistance to climate variability, we use the total number of breakpoints fitted by BFAST during the study period (1984-2011). This choice was motivated by studies that validated and tested BFAST type approaches, showing that breakpoints can be used to find drought induced trend changes (Huang et al., 2014; Verbesselt et al., 2012). Using the number of breakpoints as an inverted measure of ecosystem resistance is an innovative approach which, to our knowledge, has not been used in previous studies. As a proxy for the recovery rate of the vegetation after a drought, we used the modelled linear slope of the NDVI (henceforth "NDVI recovery trend"), succeeding breakpoints that occurred during a prolonged dry period (hydrological years 2005 to 2008 from 01.10.2004 until 30.09.2008). Our research objectives were: 1) to quantify and map ecosystem resistance to climate variability and the recovery rate after a drought (total number of breakpoints, NDVI recovery trend) in our study area, and 2) to analyse the spatial distributions of our measures for resistance and recovery in relation to grazing intensity, mean NDVI, terrain slope and aspect.

In our study area, we assumed that climatic forces were the main driver of breakpoints, because besides grazing no other temporal causes of changes in vegetation dynamics were known by local land users. We expected that the likelihood of individual pixels to experience a breakpoint (i.e. our inverse measure of resistance) and the recovery after a drought would be affected by the spatial variation of grazing intensity and environmental factors. We assumed that a healthy ecosystem has a higher resilience (being resistant and recovering fast) to climate variability than a degraded one. Regarding our proxy for recovery rate after drought, we expected a negative relationship with all factors that promote degradation in our study area, namely a high grazing intensity, a southern orientation and steep slopes. The same holds true for the mean NDVI, which can serve as a relative inverted proxy for degradation related to a loss of vegetation cover. When looking at the spatial density distribution of resistance to climate variability, we expected a bimodal shape with regard to the degradation state of the ecosystem (Figure 1): pixels with few breakpoints (i.e. high resistance) should be overrepresented in areas that are likely to be in a healthy ecosystem state (phase C in Figure 1; associated with low

grazing, very high NDVI, shallow, northern slopes), while pixels with many breakpoints (i.e. low resistance) should be overrepresented in areas that a likely to be in transition to a degraded state (phase B in Figure 1). However, once the ecosystem has reached a strongly degraded state (associated with very high grazing intensity, very low NDVI, steep, southern slopes), or in areas with rocky surfaces, it cannot react to climate variability any longer (phase A in Figure 1). In such an unresponsive ecosystem state, we also expected an overrepresentation of pixels with no or one breakpoints (i.e. high resistance); yet in this case high resistance would not be an indication of ecosystem health, and would be expected to occur in combination with a low recovery rate.

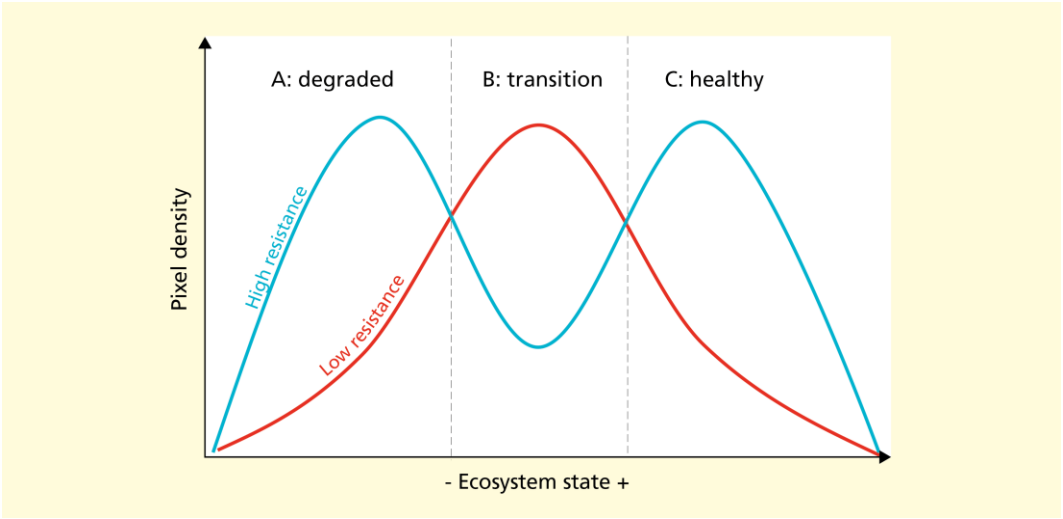

Figure 1. Graphical hypothesis of resistance related to ecosystem state. The spatial density distribution of Landsat pixels representing high resistance were expected to show a bimodal pattern with regard to ecosystem state (blue line). Maxima were expected at a strongly degraded (phase A) as well as at a very healthy (phase C) ecosystem state. Pixels representing areas with low resistance (red line) were expected to be concentrated at intermediate ranges of ecosystem health, associated with areas in transition between states (phase B).

Our hypothesis about resistance and recovery with regard to the degradation state of the ecosystem is supported by López et al. (2013). They suggested that a healthy ecosystem state would be associated with high resistance in combination with high recovery potential; beyond a critical threshold the ecosystem would become unstable, which would be associated with a reduction in resistance and recovery potential; in a highly degraded state the ecosystem would reach an indifferent stable dynamic

equilibrium, which would be associated with enhanced resistance to a disturbance factor, but with loss of recovery potential (López et al., 2013). Our hypothesis is further in line with the two steady state model by Noy-Meir (1975), where there is a stable/resistant state with regard to grazing at high plant biomass as well as at low plant biomass (in the later phase, most of the soil is bare and only less palatable plant species are present). Between those two stable/resistant states is a “turning point” where the ecosystem has low resistance.

2. Materials and Methods

2.1. Study Area

The study area, Randi Forest, is located in southern Cyprus, near Pissouri town (34°40'20"N 32°38'50"O). The area was originally a pine woodland, which was cut around 1930 (pers. comm. local farmer). Since then, the area is covered by an open shrubland with mosaics of vegetation patches including some grasses. It is grazed mostly by goats, but also some sheep. There is a wide diversity of shrubs both palatable (e.g. Sarcopoterium spinosum) and unpalatable (e.g. Urginea maritima). Woody vegetation in the area consists mainly of small bonsai-type shrubs. This shape is caused by the goats that eat the outer palatable sprouts while avoiding the thorny inner parts. Palatable perennial herbs mainly grow within thorny shrubs, thereby being protected from grazing. The diversity of annuals is large, including small grasses, legumes and forbs. The area is not owned by the shepherds, but they are commons open to all. Since the 1970s grazing pressure has strongly increased, due to a growing tourism development and coastal urbanization in the Pissouri district, which reduced the total area available for livestock grazing. This development has led to strong overgrazing in the Randi Forest (Daliakopoulos and Tsanis, 2014).

The climate is Mediterranean: summers are dry and hot, while winters are relatively wet (see Figure S1 for monthly rainfall and temperature). The average annual rainfall in our study period (1.10.1983-30.09.2012) was 396 mm. Mean daily maximum temperature varies between 30°C (July and August) and 17°C (January and February). In the last decades there has been an increasing trend in aridity due to rising temperatures and a higher frequency of years with low precipitation and drought (Republic of Cyprus: Meteorological Service, 2019). The soils are derived from marls and are shallow Calcaric Regosols (IUSS Working Group WRB, 2015) with a light colour and high calcium carbonate content (60-70%). The area is moderately hilly with an elevation between 65 and 281 m above sea level. Most

hillslopes range between 10° and 20° and are predominantly facing south-west (based on SRTM v3.0 digital elevation model).

Based on interviews with local farmers, we selected our area of interest. In our study area, there used to be seven farms (Figure 2). According to the farmers, the goats usually walk a maximum distance of 800 meters away from the farms. Therefore, we included everything within a 1000 m distance from the 7 farms (using an extra buffer of 200 meter). Between 2000 and 2006, a highway was built. To exclude disturbances by this road, we excluded the area at the southern side of the highway that blocked cattle from accessing this area. Further, we drew a circle with a radius of 800 m around a farm north of our study area. This region was excluded to eliminate the influence of this farm. This selection process resulted in our area of interest (Figure 2), covering 3.1 km^2 (3439 Landsat pixels).

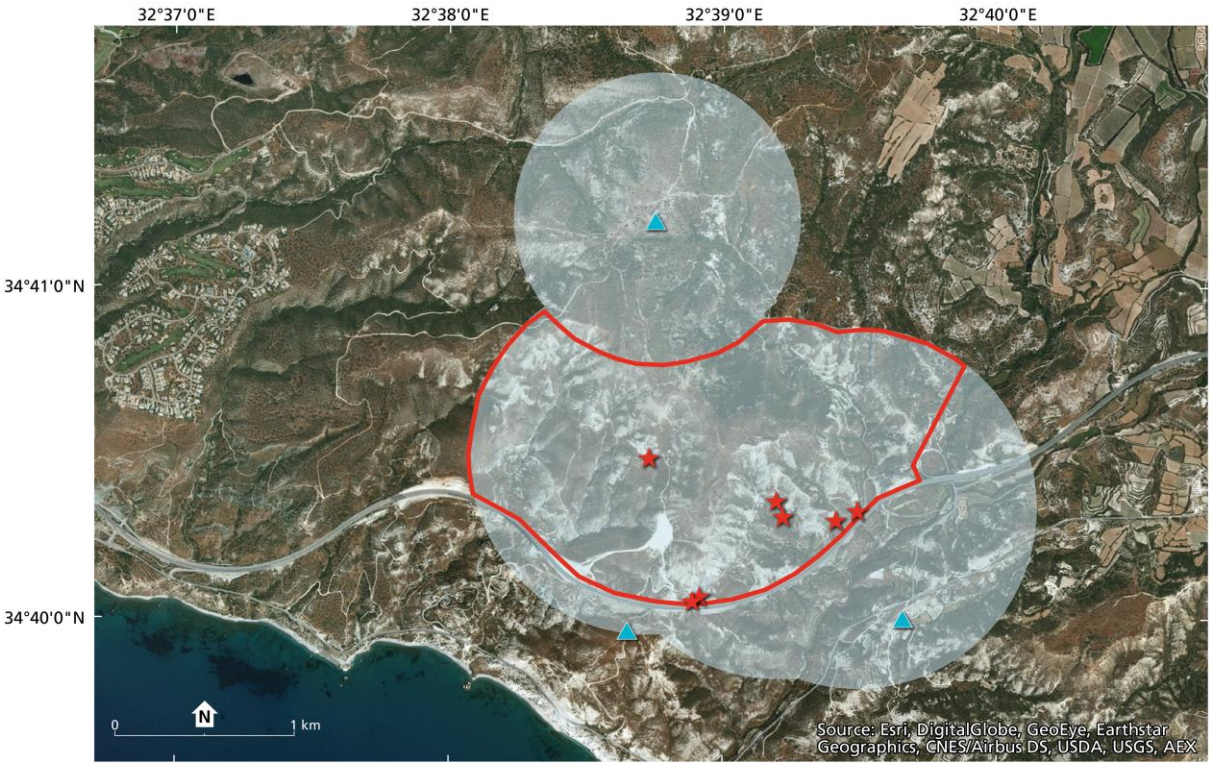

Figure 2. Area of interest (3.1 km^2, 3439 Landsat pixels). Red stars show all 7 farms in the area of interest. Blue triangles represent farms outside the area of interest. Grey circles of 1000 m radius are drawn around the farms of interest to show the grazing area related to those farms. Final area for the grazing study is outlined in red.

2.2. Satellite data acquisition and data pre-processing

This study makes use of all available Landsat 5 and 7 data available for the time period 1984-2011. The spectral response functions of the bands required for the calculation of the NDVI of the TM and ETM+ sensors aboard Landsat 5 and 7 are almost identical. This allows inter-sensor comparability of the information collected by these bands, which is essential when aiming at time series analysis that is by nature highly sensitive to external error sources. Landsat TM, ETM+ data are collected decentralized via several ground stations around the globe. Both the archives from the U.S Geological Survey (USGS) and the European Space Agency (ESA) have acquired a comprehensive collection of Landsat scenes, which are available for free download. However, the data collections in neither archive are complete, and at the time of our study, at WRS-II path/row 176/36, most scenes from the 80s were only available in the ESA archive. We therefore downloaded all available level-1 ground-terrain-corrected TM and ETM+ (excluding SLC-off) Landsat imagery (542 scenes in total) from the ESA archive for the time period 1984-2011.

The collected data was atmospherically corrected to surface reflectance using the Landsat Ecosystem Disturbance Adaptive Processing System (LEDAPS, version 2.7.0) (Masek et al., 2006; Schmidt et al., 2013). All scenes were included independent of total cloud cover, but subsequently pixels affected by clouds, cloud shadow, snow and missing data were masked out on pixel level based on the "QA" layers produced by LEDAPS. Hence, the total number of valid observations used for our analysis varies slightly within our study area (Figure S2). Since we found that there were geospatial shifts in the sub-pixel range present in the data that would hamper multi-temporal analyses, all scenes were geospatially co-registered to a master scene using the software AROSICS (Scheffler et al., 2017). For details about the coregistration with AROSICS see S2. Finally, several erroneous scenes were sorted out, e.g. scenes where the co-registration failed due to high cloud cover, or scenes that were shifted over the sub-pixel range. In total, 476 Landsat scenes (414 TM and 62 ETM+ scenes) were included in our analysis (Figure S3). On average we have 17 (± 6.3 SD) scenes per year. There are no extensive data gaps in the time

series but temporal image density varies (Figure 5F). In 1999 to 2002 image density is higher than the average, while in 1990 and 2003 very few images were available. All datasets were projected to UTM (Universal Transverse Mercator) coordinate system zone 36N (WGS 1984).

2.3. Change detection in NDVI time series and extraction of proxies for resistance and recovery

We chose the NDVI as a climate driven indicator of ecosystem dynamics. Regarding the effect of the choice of vegetation index on BFAST performance, a study by Watts and Laffan (2013), which used NDVI and the Enhanced Vegetation Index (EVI) in a BFAST time-series analysis in a semi-arid environment, concluded that there was no clear advantage in using one particular index. Here, NDVI is used as a proxy for physical vegetation properties like fraction cover or biomass. NDVI is similarly frequently used in other studies in a range of environments including drylands (Vicente-Serrano et al., 2013; Watts and Laffan, 2013) because of its strong relation to structural and functional characteristics of vegetation (Gaitán et al., 2013; Simoniello et al., 2008) and its simplicity in use.

The NDVI was calculated for each scene, resulting in an irregular time series for each pixel of our study area. Additive season-trend models were fitted to our data as described in detail in Verbesselt et al. (2010b), using the R package “bfast” (Verbesselt et al., 2012, 2010a, 2010b), where the data are decomposed into a linear trend and a harmonic, seasonal part. Since our time series is irregularly spaced, we used a frequency of 365. To describe the seasonality in our data, we used three harmonic terms. Using a higher order resulted in over-fitting, while a lower order did not adequately capture the intra-annual variation in our data.

To detect breakpoints in the time series, we followed the “breakpoint” approach originally described in Bai & Perron (1998) and implemented in the R package “strucchange” by Zeileis et al. (2003, 2002). First, an ordinary least squares (OLS) residuals-based Moving Sum (MOSUM) test was performed to test for a deviation from structural stability. If the MOSUM test was significant (p-value <0.05),

breakpoints were fitted. The optimal number of breakpoints was determined by minimizing the Bayesian Information Criterion (BIC) and the position of the breakpoints (breakdates and confidence intervals) were chosen by globally minimizing the residual sum of squares. The parameter “h”, which sets the minimum number of observations required between two breakpoints, was set to 0.15, based on recommendations in Bai and Perron (1998) as well as Watts and Laffan (2013); the latter found an advantage of using h values of 0.2 or smaller. With our 476 scenes, setting “h" to 0.15 results in a minimum of 71 scenes (approximately 3.4 years, depending on data availability and cloud conditions) between two breakpoints. The total number of breakpoints and their time of occurrence for each pixel was extracted and saved for further analysis.

To study how the NDVI recovery trend after a drought was affected by grazing and topographic properties, we selected pixels that experienced a drought-associated breakpoint in the hydrological years 2005 to 2008 (01.10.2004-30.09.2008) on a pixel by pixel basis. During this time period, a majority (77%) of the pixels in the study area experienced at least one breakpoint (Figure 5D). This widespread occurrence of breakpoints throughout our study area cannot be explained by small-scale disturbances or local land use change, nor by temporal variation in data availability. A denser time series increases the likelihood to detect a breakpoint, yet it is not above average during the time period in question (Figure 5F). Climatic drivers, however, affected the area as a whole. The hydrological years 2005 to 2008 (01.10.2004-30.09.2008) were relatively dry, including two major droughts (2006 and 2008). This dry period was preceded by three successive wet years (from 2002 until 2004) (Figure 5E). In this study we therefore assume that the widespread occurrence of breakpoints throughout our study area between 2005 and 2008 was driven by drought. To make this assumption more robust, we calculated the relative change in the mean NDVI of the three years before and after the breakpoint. Only if the NDVI dropped by at least 10% the pixels were included in the further analysis (81% of all breakpoint pixels). In the rare case that more than one breakpoint was found between 2005 and 2008 the first one was selected for further analysis. Additive season-trend models (Verbesselt et al., 2010b) were fitted to the segment after the breakpoint, using the robust regression approach described in

DeVries et al. (2016) that is particularly robust to outliers. The slope of the linear trend component was extracted from the model parameters and used as a measure for the recovery rate of the vegetation after a drought ("NDVI recovery trend").

Finally, maps of the number of breakpoints and the NDVI recovery trend, together with the location and size of the farms in 1987 and terrain contour lines, were produced for our study area. All satellite data processing steps are summarized in Figure 3. The code for the adapted BFAST analysis and for extraction of the number of breakpoints and NDVI recovery trend can be found at "https://github.com/jennifervk/resInd".

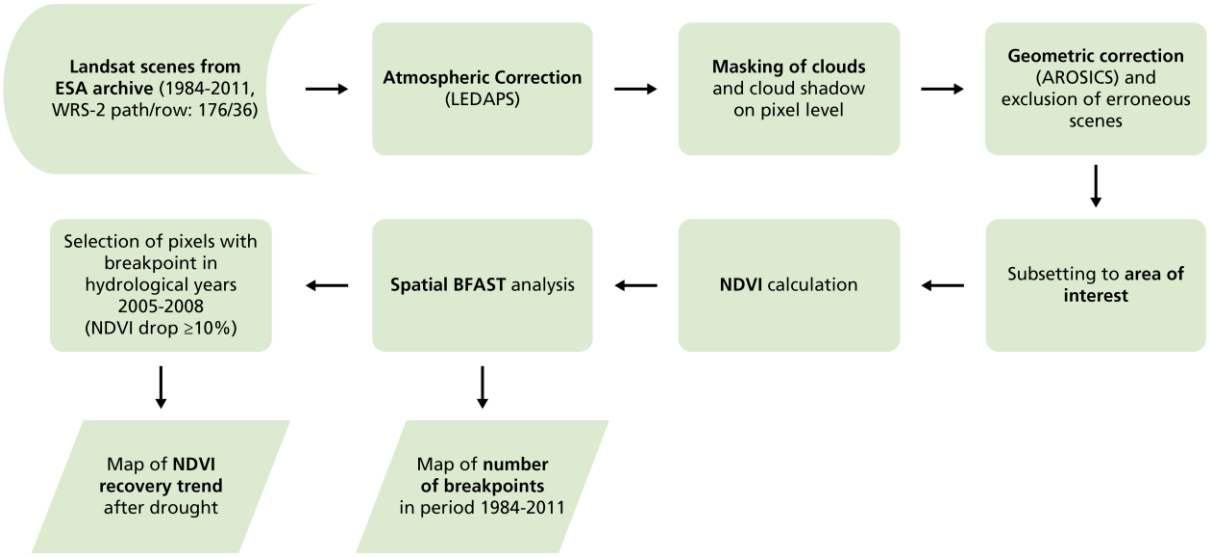

Figure 3. Scheme of the satellite data processing steps.

The BFAST analysis, together with two high resolution satellite images taken in August 2003 and 2009, is shown for three exemplary Landsat pixels (A, B, C) located in the south of our study area (Figure 4 & Figure 5 A-C). The pixels show varying dynamics: pixel A is located on a southeast-facing slope with few shrubs, little grass cover and visible rill erosion (Figure 4). It has three breakpoints (i.e. low resistance), and a low NDVI recovery trend after the breakpoint in 2005 (Figure 5A). This combination indicates low ecosystem resilience. Compared to pixel A, pixel B has higher vegetation cover that also contains

an herbaceous layer (Figure 4). It has only two breakpoints and shows a steeper recovery trend after the breakpoint in 2006 (Figure 5B). This combination indicates higher ecosystem resilience compared to pixel A. Pixel C mostly contains bare soil (Figure 4) and has no breakpoints (Figure 5C). This pixel represents the almost barren, unresponsive state, for which we expected no or one breakpoint.

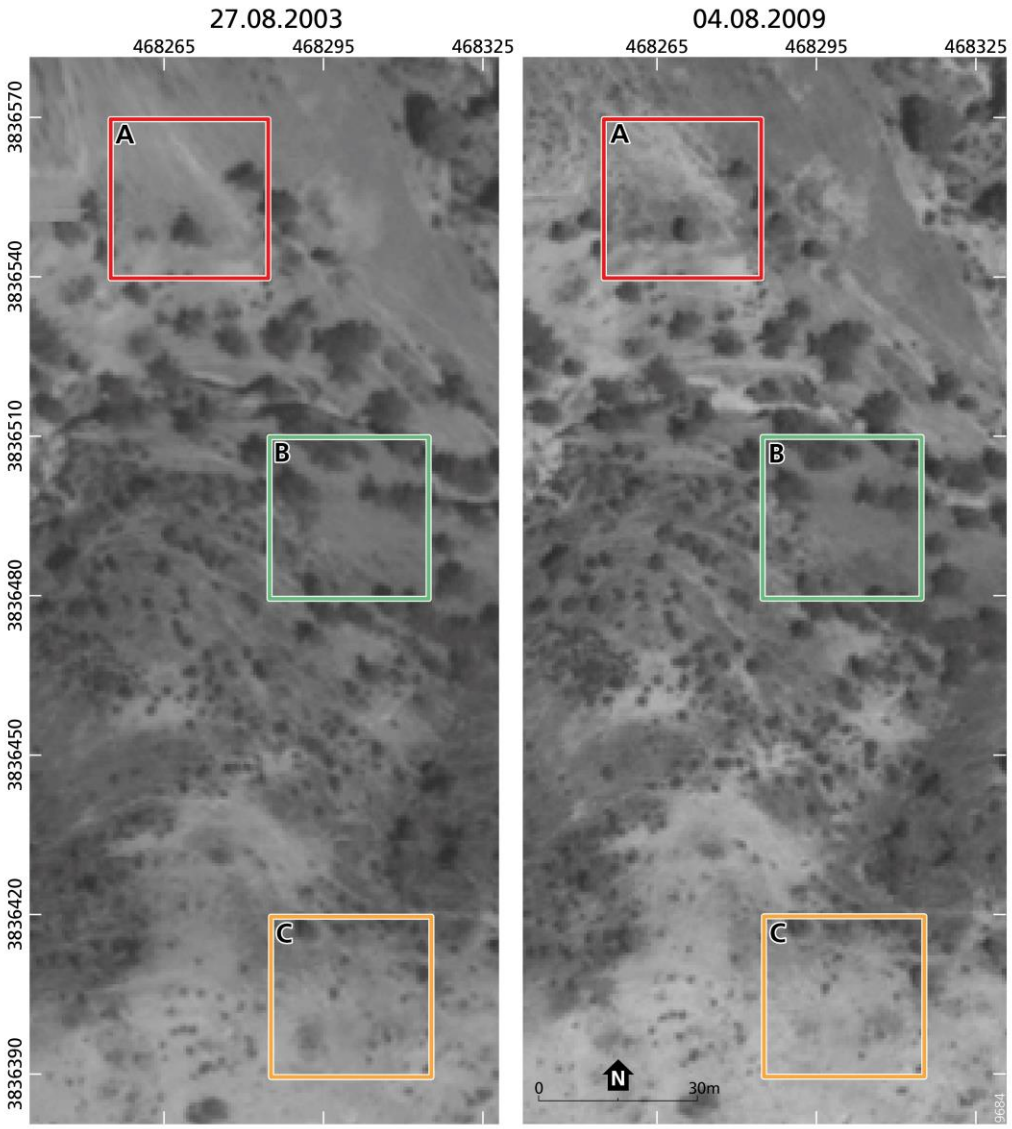

Figure 4. Example 30x30 m Landsat pixels A, B & C. Two Quickbird images (panchromatic, spatial resolution: 0.6 m) taken on 27.08.2003 and 04.08.2009. Results of BFAST analysis for pixels A, B & C are shown in Figure 5 A-C.

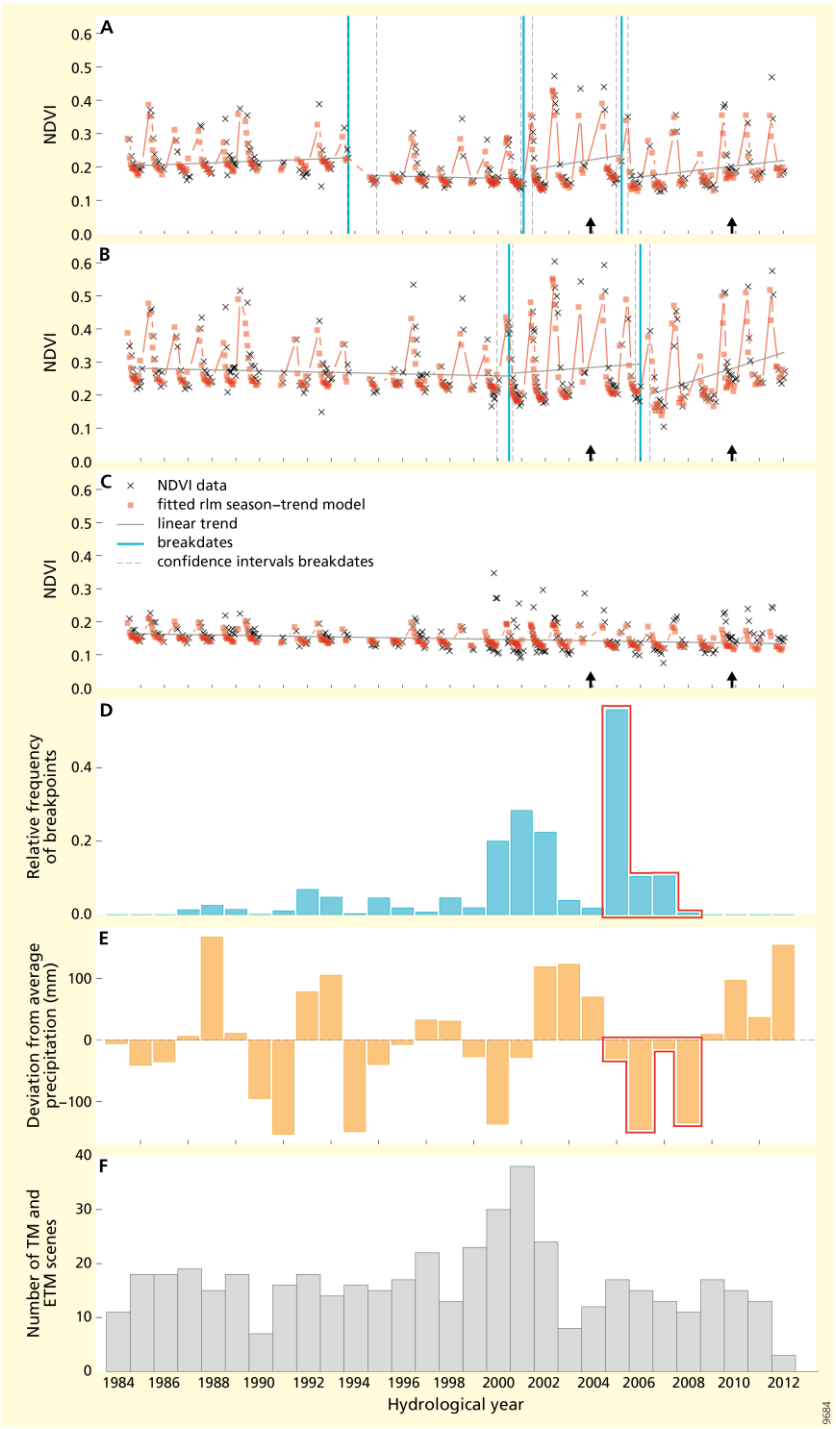

Figure 5. BFAST results for example pixels A, B, C. The two arrows indicate the time point of the Quickbird images shown in Figure 4. Relative frequency of breakpoints (D) and rainfall anomaly (μ = 396 mm, SD = 92 mm) (E) in the study area for the hydrological years 1984-2012. The red borders around the bars in E and F indicate the period of drought (hydrological years 2005 - 2008) that was selected to study the NDVI recovery trend after a drought breakpoint. (F) Number of available TM and ETM+ (excluding SLC-off scenes) scenes from the ESA archive that were included in the analysis. All scenes irrespective of cloud cover were included; clouds and cloud shadows were masked on pixel level.

2.4. Topographic properties and grazing

Both aspect and terrain slope can affect the vegetation resilience to climate variability. We obtained these topographic properties from the digital elevation model provided by the Shuttle Radar Topography Mission (SRTM v3.0) at a spatial resolution of 1 arc-second. To align the elevation cells with the Landsat raster, a bilinear resampling was performed in ArcGIS 10.6.1. Thereafter, aspect (in degrees) and terrain slope (in %) were obtained with the ArcGIS Spatial Analyst Toolbox.

Grazing by goats affects the vegetation dynamics both directly, by reducing vegetation cover, and indirectly, by trampling. In this paper, we look at the combined effects without differentiating between direct and indirect aspects. Local farmers were interviewed to estimate the grazing intensity in our study area. The farmers explained that the goats can walk freely throughout the study area during several hours of the day throughout the whole year. The farmers occasionally give additional fodder, mainly in summer, due to sparse palatable vegetation in this season. The amount of fodder given varies a lot between year and season. The animals prefer to stay close to the farm, so our estimated grazing intensity decreases with the distance to the farm. The farmers also explained that when the animals want to reach an area up- or downhill, they do not walk straight uphill. Instead, they have created walking paths along the hills, thereby increasing the distance to walk uphill. We received information about the number of animals for each of the seven farms around 1987 and 2007, respectively.

This information from the local farmers was used to estimate the relative grazing intensity (livestock/m) for each 30x30 m pixel (x,y) with the path distance tool in ArcGIS. As input variables, we used the number of animals per farm (i) and the distance between the pixel and the farm:

$$Grazing\ intensity_{x,y} = \sum_{i=1}^{n} \frac{animals_i}{distance_{i(x,y)}}$$

This calculation is in agreement with other studies (e.g. Manthey and Peper 2010), which show that grazing can be estimated by the inverse distance from a hotspot, which is in our case the farm. A vertical friction factor (symmetric inverse linear with the default slope of -1/45 in ArcGIS) was added

to the distance to represent the extra 'friction' for the goats to walk up- or downhill as explained by the local farmers. The distribution of estimated grazing intensity is strongly right skewed. Therefore, we removed all grazing values above the 97.5% quantile. These calculations resulted in estimations of the grazing intensities for both 1987 and 2007 (S4). Our estimates of 0-9 livestock/m are in the same range as found in another semi-arid rangeland by Manthey and Peper (2010). For the statistical analysis of the NDVI recovery trend, we have log-transformed the grazing intensities with $log\ (grazing\ intensity - 1)$. This transformation gave the best approximation to a normal distribution.

2.5. Data Analysis

To study the relationship between grazing intensity, terrain slope, aspect, mean NDVI and the number of breakpoints spatially on a pixel by pixel basis, we sorted all pixels into breakpoint categories from zero to four. Pixels with five breakpoints were excluded, because only two pixels were in this category. The mean NDVI was calculated based on all available observations between 1984 and 2011 for each individual pixel.

We calculated the spatial Kernel probability density distributions of each breakpoint category over grazing intensity, mean NDVI, terrain slope and deviation from south (i.e. deviation from maximum solar radiation), and compared them to the overall distributions of these variables in our study area. We assumed that a random sample of pixels should not deviate considerably from the overall distribution of the studied variable; if a distinct deviation can be observed, it must be caused by some mechanism related to that variable. A two-sample Kolmogorov-Smirnov test (henceforth "KS-test") was performed to test against the null hypothesis that the breakpoint categories were drawn from the same underlying continuous distributions as the overall distributions of the respective variables in our study area, using the R package "stats" (R Core Team, 2017) at a significance level of $\alpha = 0.01$. To visually highlight the differences to the overall distributions of grazing intensity, mean NDVI, terrain slope and aspect, we divided the density of each breakpoint category (estimated at 1000 equally

spaced points between the min. and max. data ranges), by the overall density of the studied variables in our study area, keeping the bandwidth for estimating the smoothing kernels constant. We thus created a “Relative Density Breakpoint Index (RDBI)”:

$$RDBI_i = \frac{DB_i}{D_T} \text{ with } i = \{0, \ldots, 4\}$$

DB stands for the density of the respective breakpoint category (i) and D_T for the overall density of the studied variables in our study area. A value of 1 signifies no difference to the overall distribution of the studied variable; a value larger than 1 signifies an overrepresentation of the breakpoint category at this data range and a value below 1 an underrepresentation.

To study the relationship between the NDVI recovery trend, grazing, topographic properties and the mean NDVI in the three years before the breakpoint, we applied generalized linear regression analysis with the “gls” function in the “nlme” package in R (Pinheiro et al., 2018). Scaled factors were used to obtain the ß-values. Spatial autocorrelation is present in the data. We tested six autocorrelation structures within the “gls” function, namely exponential, gaussian, spherical, linear and rational quadratic. In all cases, the rational quadratic models had the lowest AIC values and were therefore used for our analysis.

3. Results

3.1. Spatial distribution of breakpoint categories and NDVI recovery trend

Between 1984 and 2011, pixels experienced between zero and five breakpoints in our study area (3439 pixels in total). 41.6% pixels had two breakpoints, followed by one breakpoint (29.1%), three breakpoints (18.6%), zero breakpoints (6.4%), four breakpoints (4.2%) and five breakpoints (0.1%). The spatial distribution of the number of breakpoints shows a large variability, with some breakpoint classes appearing more clustered (0, 4, 5), and others (1, 2) more evenly distributed in the whole area (Figure 6A).

In the relatively dry hydrological years between 2005 and 2008, 77% of the pixels in the study area experienced at least one breakpoint (Figure 5D). Of those breakpoints, 81% were associated with a relative decrease in NDVI of at least 10%. Following this decrease in NDVI, nearly all pixels (99.7% of the pixels experiencing a decrease in NDVI of at least 10%) showed a positive NDVI recovery trend, although there was a large spatial variability in the magnitude of the NDVI recovery trend (Figure 6B).

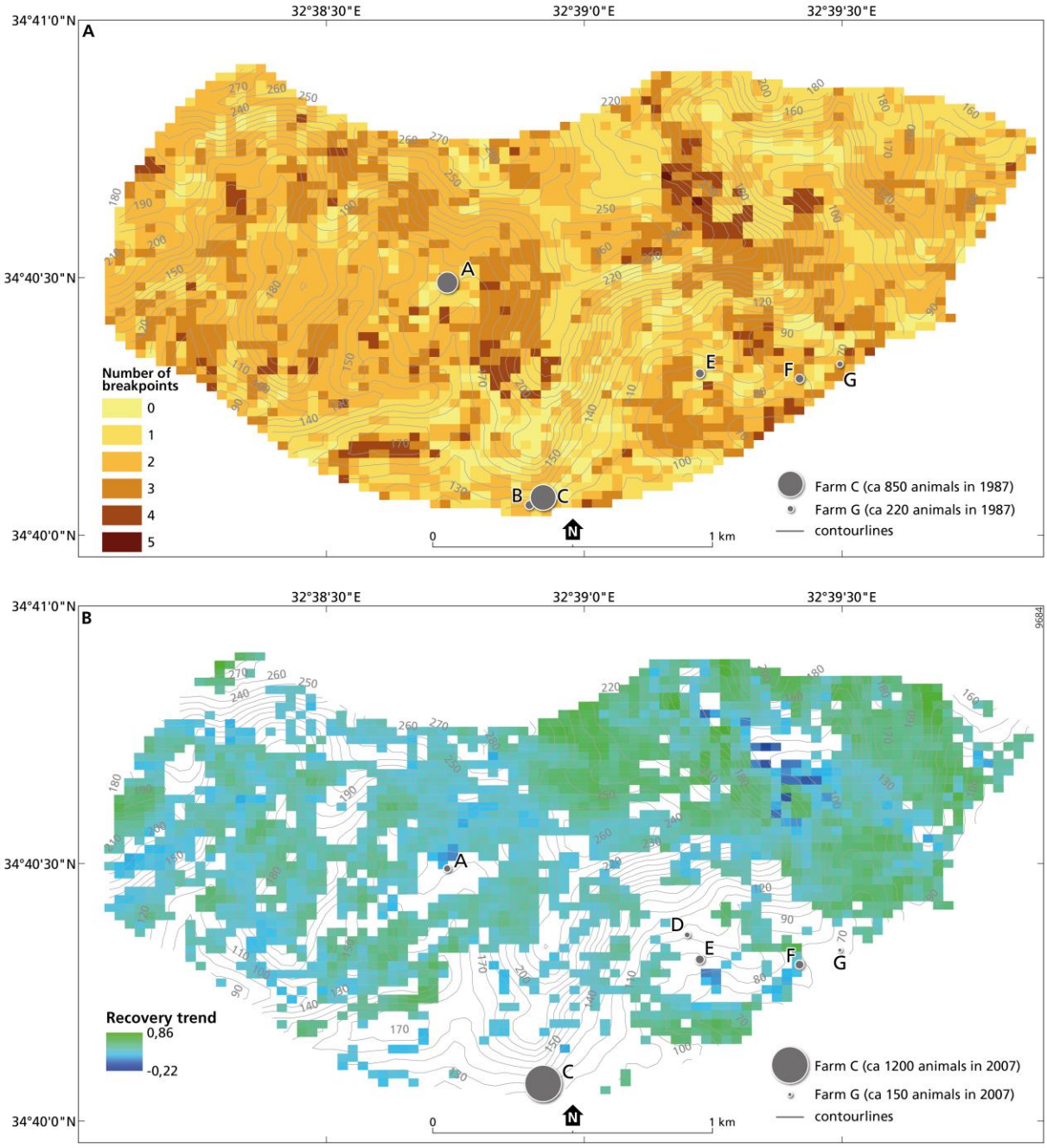

Figure 6. (A) Number of breakpoints fitted by BFAST on pixel basis in the period 1984-2011. Circles depict goat farms with the size of the circle proportional to the estimated number of animals in 1987. (B) NDVI recovery trend ($\frac{\Delta NDVI}{day} \times 10{,}000$) after the 2005-2008 relatively dry hydrological years for pixels that experienced a breakpoint in this time period. Results are only shown for pixels that experienced a relative decrease in NDVI of at least 10% using average NDVI of the three years before and after the breakpoint. Circles depict goat farms with the size of the circle proportional to the estimated number of animals in 2007.

3.2. Analysis of breakpoint category distributions in relation to spatial patterns of topographic properties, mean NDVI and grazing intensity

The 1- and 2-breakpoint categories dominate over all data ranges of grazing intensity, mean NDVI terrain slope and deviation from south (i.e. deviation from maximum solar radiation) (Figure 7 A-D). The relative density distributions of the individual breakpoint categories discernibly differ in shape (Figure 7 E-H): while some follow the shape of the overall distributions of the studied variables, others deviate clearly from the latter, indicating that their behaviour in relation to that variable is not random. The distribution of the 2-breakpoint category was not affected significantly by any of the variables, which fits to the visual impression that this category appears randomly spread in space (Figure 6A).

For grazing intensity, the distributions of the 0-, 3- and 4-breakpoint categories differed significantly from the overall distribution in our study area (KS test, α=0.01; Table S5). When interpreting the results of different grazing levels, one has to note that the distribution of grazing is strongly right skewed (Figure 7A). Thus, we used the 25% and 75% quantile to differentiate between low (<1.8), medium (1.8-2.8) and high (>2.8) grazing intensities. Relative to the overall distribution of grazing intensity (Figure 7E&I) the 0-breakpoint category is particularly overrepresented at high to very high grazing levels, corresponding mostly to areas in the vicinity to farms. The 3-breakpoint category is slightly overrepresented at high grazing levels and the 4-breakpoint category is overrepresented at different ranges from medium to high grazing levels.

For mean NDVI, the distributions of the 0-, 1- and 3-breakpoint categories differed significantly from the overall distribution in our study area (KS test, α=0.01; Table S5). Relative to the overall distribution of mean NDVI (Figure 7F&J) the 0-breakpoint category is strongly overrepresented at low NDVI levels (< 0.2), the 1-breakpoint category at extremely low (< 0.16) as well as extremely high (> 0.27) NDVI values, and the 3-breakpoint category at medium NDVI values.

For the topographic properties, only aspect showed significant results. The distributions of the 1- and 3-breakpoint categories differed significantly from the overall distribution of aspect (measured as

deviation from south) in our study area (KS test, α=0.01; Table S5). The 1-breakpoint category was overrepresented on northern slopes, the 3-breakpoint category on western slopes.

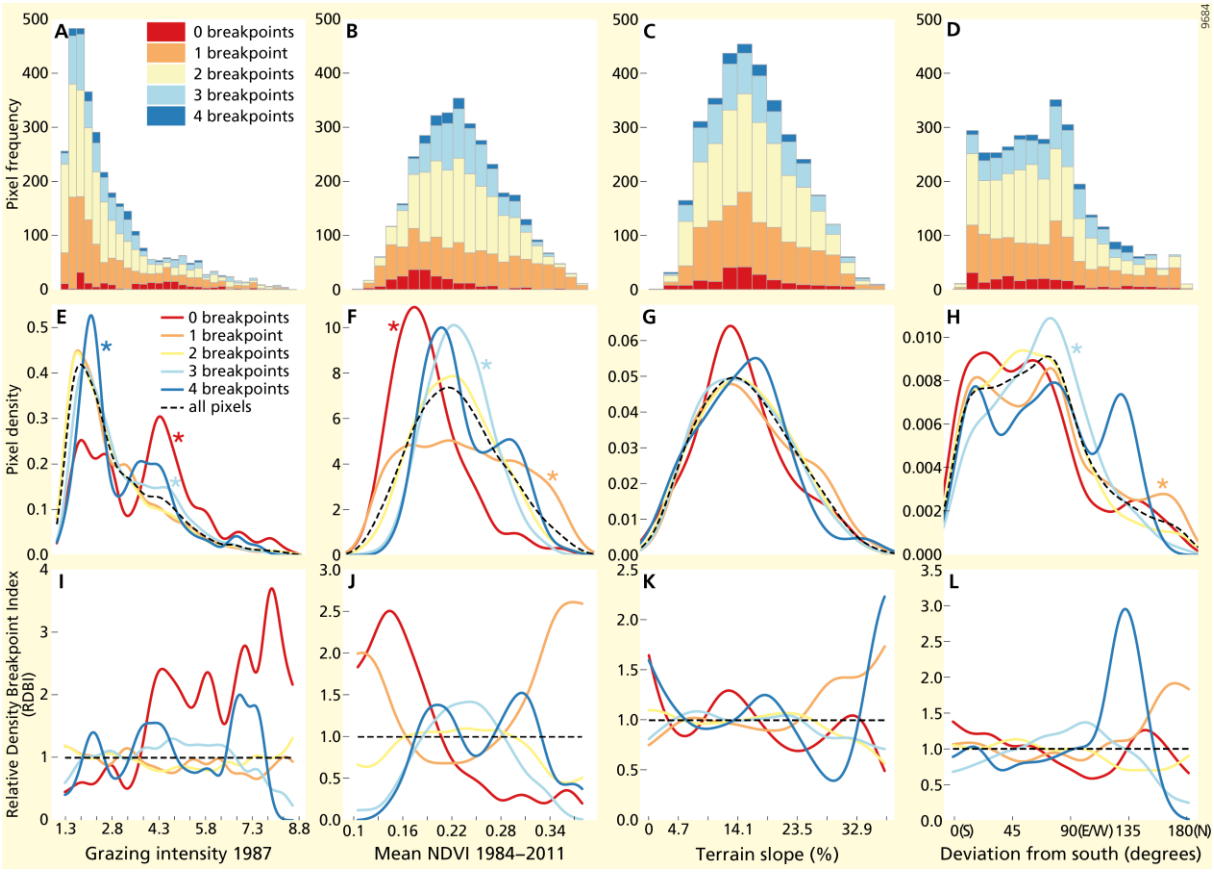

Figure 7. Spatial distributions of breakpoint categories over grazing intensity 1987 (livestock/m), mean NDVI 1984-2011, terrain slope and deviation from south. Number of pixels in each breakpoint category: 0 breakpoints: 220, 1 breakpoint: 1001, 2 breakpoints: 1432, 3 breakpoints: 639, 4 breakpoints: 145, total: 3439. A-D: stacked frequency histograms of breakpoint categories showing absolute numbers of pixels. E-H: kernel density estimations for each breakpoint category separately and for all pixels combined (bandwidth=0.27 (E), 0.01 (F), 2.50 (G), 9.91 (H)). Breakpoint categories for which the KS test indicated a significant deviation (α = 0.01) from the overall distribution are marked with a star. I-L: Relative Density Breakpoint Index ($RDBI_i$): the densities of the breakpoint categories $i = \{0, \ldots, 4\}$ divided by the overall density of grazing intensity, mean NDVI, terrain slope and deviation from south. Note that the RDBI is a relative measure that only applies to the distribution of the data within each category in relation to the overall distribution of the studied variable.

3.3. The effect of grazing and topographic properties on the NDVI recovery trend

To study what affects the recovery after the drought between the hydrological years 2005 and 2008, we used linear regression models. The simple linear regression shows that there is a clear positive relation between the mean NDVI three years before the breakpoint and the NDVI recovery trend after the breakpoint (Figure 8A). This relationship indicates that 'greener' pixels recover faster. However, no significant relationship (α=0.05) was found between terrain slope and the NDVI recovery trend (Figure 8B). A significant relationship has been found between aspect and the NDVI recovery trend (Figure 8C). Namely, southern pixels have a low NDVI recovery trend, while the recovery trend significantly increases when the orientation turns towards north (Figure 8C). This relationship indicates that northern-oriented pixels recover faster. The grazing intensities for 1987 (Figure 8D) and 2007 (S6B) have a slightly negative relationship with the NDVI recovery trend.

When combining all factors that could explain the NDVI recovery trend after the breakpoint in one multiple regression model including significant interaction factors (using backward elimination), the relationships have a similar direction and two significant interaction factors were found (Table 1). The variance inflation factor (VIF) was below 1.6 among factors, indicating that there is low multicollinearity between the explanatory factors. The most significant interaction factor is between aspect (measured by deviation from south) and terrain slope. While the NDVI recovery trend was not significantly related to terrain slope when using simple linear regression (Figure 8B), this relationship changes when including aspect (Figure 9A). The relationship between NDVI recovery trend and terrain slope is positive for northern-oriented slopes, while it is negative for southern-oriented slopes. Thus, on northern slopes, terrain slope has a positive effect on the NDVI recovery trend, while on southern slopes it has a negative effect. The second interaction factor is between deviation from south and the mean NDVI before the breakpoint. In the simple linear regression, there was a significant positive relationship between the deviation from south and the NDVI recovery trend (Figure 8C). Yet, when

grouping the data based on the upper and lower 25% of NDVI values, this positive relationship was only significant for the group with the low NDVI data (Figure 9B).

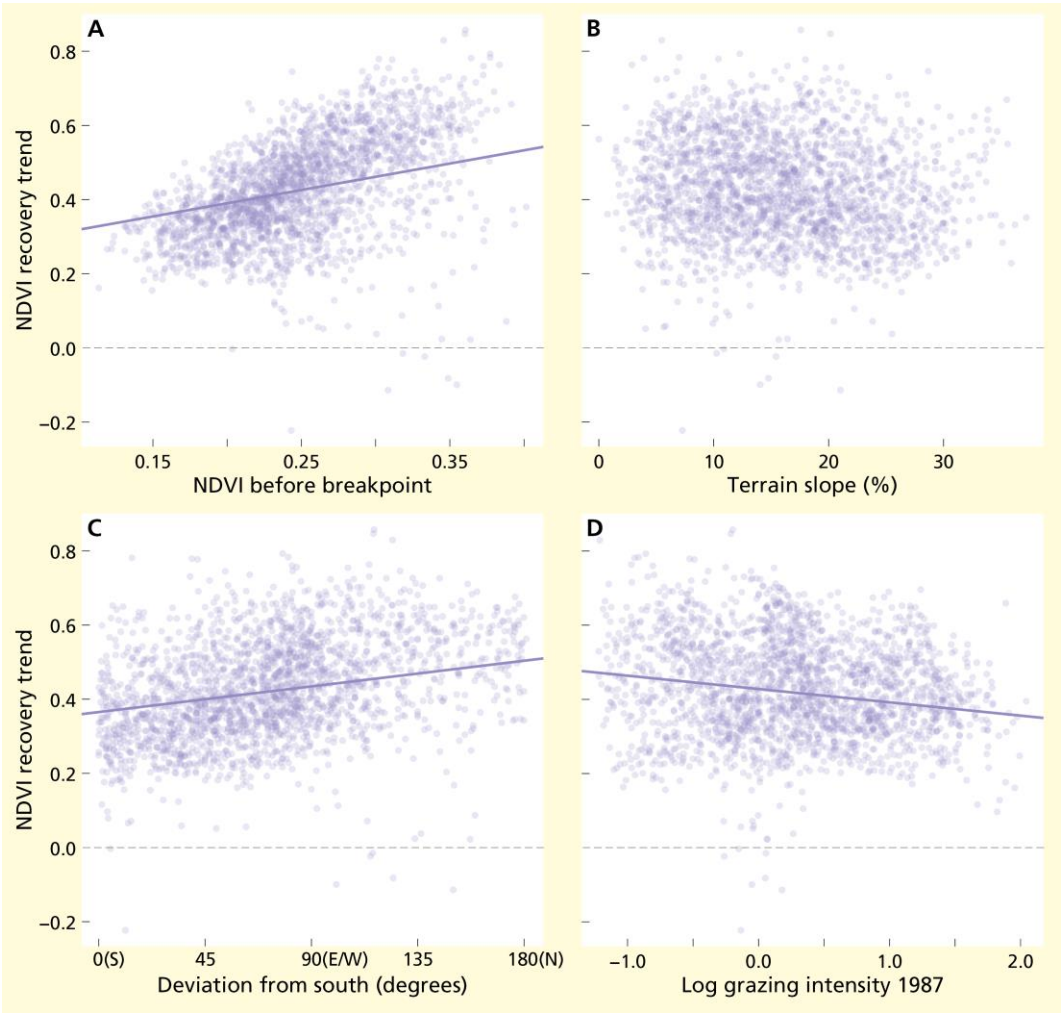

Figure 8. Simple regression analysis between the NDVI recovery trend ($\frac{\Delta NDVI}{day} \times 10{,}000$) and A) NDVI before the breakpoint (β=0.278, p<0.001) B) terrain slope (β= 0.003, p=0.932) C) aspect measured as deviation from south (β=0.242, p<0.001), D) estimated grazing intensity in 1987 (β=-0.192, p=0.010). Regression lines are shown for significant relations (α=0.05). Additional regression analyses can be found in S6.

Table 1. Multiple regression between NDVI recovery trend and the independent variables including significant interactions.

Independent variable	β	p-value
Deviation from south (degrees)	0.295	<0.001
NDVI before breakpoint	0.211	<0.001
Log grazing intensity 1987 (livestock/m)	-0.121	0.0424
Terrain slope (%)	-0.005	0.866
Deviation from south*Terrain slope	0.097	<0.001
Deviation from south*NDVI before breakpoint	-0.059	0.0116

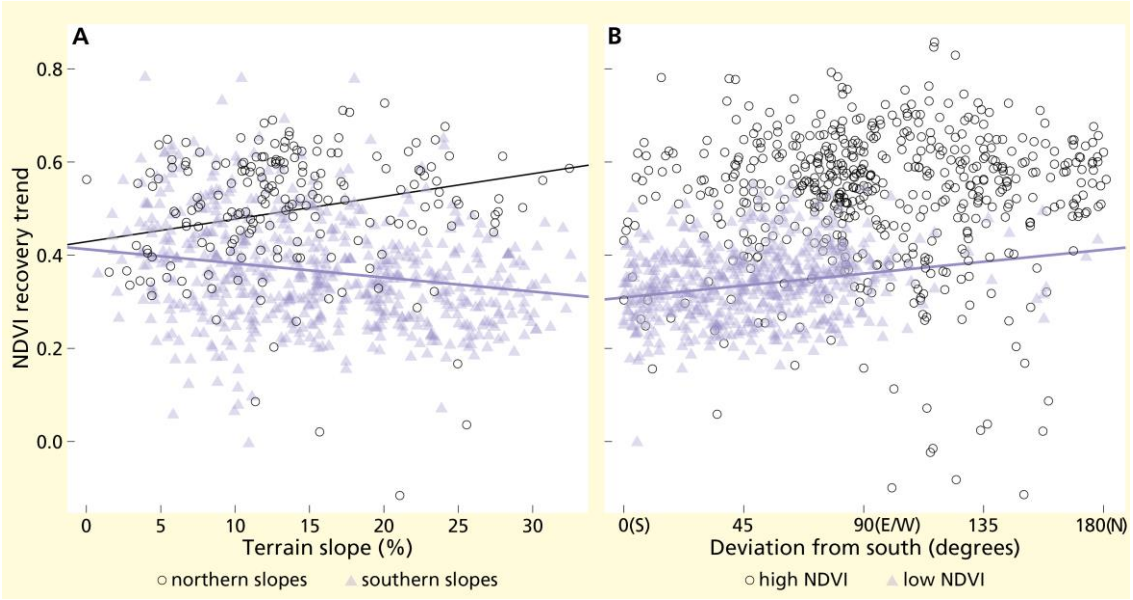

Figure 9. Simple linear regression for significant interaction factors for the NDVI recovery trend ($\frac{\Delta NDVI}{day} \times 10{,}000$) after the drought breakpoint. A) Simple linear regression between the terrain slope and the recovery trend of the NDVI after the breakpoint. The relationship is positive for northern-oriented slopes (Aspect >315° or <45° indicated by black circles, β=0.251, p=0.012), while it is negative for southern-oriented slopes (135°>Aspect<225°, indicated with blue triangles, β=-0.191, p=0.001). B) Simple linear regression between aspect (measured as deviation from south) and the NDVI recovery trend. The relationship is not significant for the 25% of the data with the highest NDVI before the breakpoint (indicated by black circles, β=0.107, p=0.105), while it is significantly positive for the 25% of the data with the lowest NDVI before the breakpoint (indicated with blue triangles, β=0.231, p<0.001). Regression lines are shown for significant relations (α=0.05).

4. Discussion

4.1. Deriving spatial indicators for resistance and recovery using a BFAST model

The first objective of this study was to quantify and map vegetation resistance to climate variation and recovery from drought using a dense irregular Landsat time series. We used the spatial distribution of the number of breakpoints fitted by a BFAST model as an inverse indicator for vegetation resistance to climate variation. The NDVI recovery trend after a drought breakpoint, derived from the BFAST model, was used as an indicator for the vegetation recovery rate. Our results (Figure 6A) show that between 1984 and 2011, zero to five breakpoints occurred on a pixel level, with most pixels experiencing two breakpoints. We thus considered pixels with zero or one breakpoint to have relatively high resistance and pixels with three or more breakpoints to have relatively low resistance to natural climatic variation such as droughts. Note that in this study resistance is not used as direct measure for ecosystem health, but that we did expect high resistance at both ends of the ecosystem state: in a very healthy, as well as in a degraded, or barren unresponsive ecosystem state. The spatial frequency of pixels with relatively high resistance (36%) exceeded those with relatively low resistance (23%). During the period of drought in 2005-2008, more than 3/4 of the pixels within our study area showed a breakpoint, and of those 99.7% displayed a positive NDVI recovery trend afterwards. These results indicate that overall our study area has a positive recovery potential and that areas with high resistance exceed those with low resistance.

4.2. Vegetation resistance and recovery in relation to grazing, mean NDVI and topographic properties

Our second objective was to study the spatial distributions of resistance to climate variability and recovery from drought in relation to controlling factors for vegetation resilience: grazing, mean NDVI, terrain slope, aspect. For resistance, the spatial distribution of the breakpoint categories related to grazing and topographic properties in our study area partially agreed with our expectations. High NDVI

and/or a northern orientation (i.e. favourable conditions) were associated with an overrepresentation of pixels with high resistance (few breakpoints). Contrary to our expectations, low grazing intensities did not significantly promote resistance. Potentially strongly degraded areas, with medium to high grazing and/or low NDVI were associated with an overrepresentation of pixels with high resistance. At variance with our expectations, a southern orientation was not clearly associated with high resistance. Intermediate conditions (intermediate grazing and/or NDVI values, and/or western/eastern slopes) were associated with an overrepresentation of pixels with low resistance (many breakpoints). Overall, this spatial pattern of resistance is in accordance with the bimodal pattern we expected for resistance related to ecosystem state: potentially healthy areas, as well as potentially degraded areas (e.g. with sparse vegetation cover) were associated with an overrepresentation of pixels with high resistance.

Regarding recovery from drought, the multiple regression analysis showed that the NDVI recovery trend was positively affected by in order of importance: a northern orientation, high NDVI values before the breakpoint and low grazing intensities (Figure 8; Table 1). These results indicate that, as expected, recovery of vegetation prevails in locations that have more favourable conditions (low stress levels by grazing and sunshine) and/or higher NDVI values and agrees with other studies: Del Barrio et al. (2010) found that trends to improve vegetation are represented most in land in good or unusually good condition, while degrading or static trends of vegetation in drylands are found to prevail in degraded or unusually degraded land. In other words, the recovery is expected to be fastest in areas where vegetation is already in a good condition.

When studying the impact of terrain slope by itself, it was neither related to resistance nor to the recovery rate. This was contrary to our hypothesis that steep slopes promote the unresponsive ecosystem state characterized by high resistance and low recovery rates. The multiple regression model revealed that there was a significant interaction between terrain slope and orientation: on southern-oriented slopes, the NDVI recovery trend was indeed negatively related with terrain slope (Figure 9A). This finding implies that the negative effects of southern orientation and steep terrain

slope were synergetic. It agrees with our expectations that southern steep slopes have low recovery rates. However, for northern-oriented pixels, the relationship between NDVI recovery trend and terrain slope is positive. This result indicates that steep terrain slope alone does not necessarily yield a permanently degraded state, but that amplifying effects by other factors are needed. A second interaction factor showed that the positive relationship between the NDVI recovery trend and deviation from south was stronger for pixels with lower mean NDVI before the drought breakpoint (Figure 9B). Thus, regarding the recovery rate, pixels with low mean NDVI before the drought breakpoint benefit more from a northern orientation than pixels with high mean NDVI. Pixels with low mean NDVI before the breakpoint are associated with scarcer vegetation and thus are more susceptible to the negative effects of strong solar radiation.

In our study, potentially strongly degraded areas (i.e. areas with very low NDVI and/or high grazing intensities) displayed low recovery rates and were associated with a strong overrepresentation of pixels with high resistance. These results conform with our hypothesis that these areas have likely reached an unresponsive permanently degraded state with no or little vegetation cover. It agrees with findings by De Keersmaecker et al. (2015), who showed that drought sensitive vegetation with a high fraction of bare soil displayed the strongest vegetation memory effects, resulting in particularly low recovery speed after a drought. Further, in a study on vegetation cover resilience in Italy (Simoniello et al., 2008), Sparsely Vegetated Areas and Pastures (i.e. potentially stressed lands) were the only Corine land cover type for which mean positive recovery trends did not exceed the negative trends during the period 1992-2003; the main clusters with a negative recovery potential were corresponding to areas at risk of desertification. Our result that strong grazing intensity promoted an unresponsive ecosystem state matches with a study by Schneider and Kéfi (2016), who found that grazing increases the bi-stability domain of a desert and a vegetated state. The authors argue that strong grazing reduces ecosystem resilience, thereby making a transition to a stable, permanently degraded desert state more likely. That strong grazing not only increases the domain of a desert state, but also makes the transition to such a state more likely, might explain why we also found a slight overrepresentation of pixels with

low resistance at high grazing intensities. Since we did not similarly find an overrepresentation of pixels with low resistance at low NDVI values, areas with low resistance that were associated with high grazing intensities do not represent a totally degraded state (with low NDVI). However, they might be in transition to a degraded state due to reduced ecosystem resilience (in our study indicated by low resistance and low recovery).

Our result that potentially degraded areas were associated with high resistance and low recovery also matches with findings by Saruul et al. (2019), who showed that highly degraded grasslands in Mongolia had high resistance to and low recovery from natural disturbances. However, in the same study moderately degraded grasslands displayed higher resistance and recovery than slightly degraded and undegraded ones. Saruul et al. (2019) ascribe their finding to positive effects of intermediate grazing levels on species composition and richness and relate it to the intermediate disturbance hypothesis. Contrarily, we found that intermediate NDVI and grazing levels were associated mostly with low resistance, and an intermediate recovery. In areas with very high NDVI however, as well as on northern-oriented slopes, we did find a significant overrepresentation of pixels with high resistance, which might indicate that these areas are in a healthy ecosystem state. That intermediate levels of grazing did not seem to have any positive effects on ecosystem resilience in our case might be ascribed to the fact that the area has been overgrazed for decades. Thus, the vegetation might not benefit from the continuation of even intermediate grazing intensities, and such areas were probably more than "moderately degraded".

In conclusion, the effects of grazing on resistance appears to depend on the ecosystem state as a whole: if highly grazed areas are associated with a strongly degraded state (in our case indicated by very low NDVI values), grazing seems to increase ecosystem resistance to climatic variation such as droughts. In this state the ecosystem cannot react to climate variability any longer. By removing vegetation cover, grazing even more promotes this state. Otherwise, strong grazing appears to lower ecosystem resistance, as also reported in a study by Whitford et al. (1999) and in De Keersmaecker et

al., (2016). Whitford et al. (1999) further found that heavy grazing reduced the recovery rate from drought, which corresponds to our results. However, the effects of grazing on resistance and recovery should be treated cautiously, since they depend on many factors. Maestre et al. (2016) pointed out that the effects of grazing on ecosystem structure and functioning in drylands vary with the intensity of grazing, the composition of herbivore assemblages, the shared evolutionary history of plants and herbivores, the way grazing pressure is measured and the spatial scale. The authors also found that grazing effects on resilience to climatic stresses are highly modulated by grazing interactions with species composition and richness. In our study area, we observed during field visits that in areas with higher grazing intensity, the number of unpalatable plant species increased. However, we did not see a clear shift in species composition from shrubs to grasses. Shrubs were the dominant vegetation type for all grazing levels. A study by Ruppert et al. (2015), who quantified drought resistance and recovery using 174 long-term datasets from more than 30 dryland regions, shows that the effects of grazing on drought resistance and recovery are modulated by the dominant life history of the herbaceous layer: in perennial systems, grazing negatively affected resistance, in annual systems it positively affected recovery. Altogether, interpreting effects of grazing on vegetation resistance and recovery across different systems and studies remains challenging.

4.3. Methodological limitations

The number of breakpoints fitted by BFAST during a given time period is a relative measure of resistance and absolute values cannot be compared between different study systems. Its interpretation depends on the overall frequency of breakpoints within the study area, which is affected by the ecosystem type, the climate regime, the duration of the study period, the spatial scale, data availability, BFAST model parameters, as well as land use and local disturbances; e.g. a total number of one breakpoint may indicate high resistance in our case, but may be indicating low resistance in another study system. It further depends on the overall aim of the study, i.e. resistance to what factor is studied.

Some considerations should be taken into account when transferring our approach to other areas. In our study, we interpret the relative occurrence of breakpoints within our study area as an inverted proxy for long-term vegetation resistance to climate variability. This interpretation presupposes that climatic forces are the main driver of breakpoints, and that the climate can be assumed to be similar in the study area. Further, it requires comparability regarding land cover type as well as land use regime (within the area). Finally, detailed knowledge about past disturbances and land use regime of the area is crucial to exclude effects of other not climate related large-scale disturbances. Our study area is relatively small, driven by the same climate regime and with a comparable land cover type and land use (a grazed dryland with mosaics of vegetation patches). The small size of our study area allowed us to combine remote sensing data with detailed information on local grazing regime. Studying resilience at a global scale would make it possible to obtain more general results (e.g. see Bernardino et al. (2020) about global-scale characterization of turning points using BFAST), but a global scale would not allow to study the local specific processes affecting resilience.

From the interviews with local farmers we gathered detailed information both about the present and the past grazing regime, which allowed us to derive a spatially explicit grazing intensity index. We learnt that no major land use change or large-scale disturbance has occurred within our area during our study period except grazing. Hence, we considered it valid to assume that main driving force of the NDVI dynamics acting on the area as a whole were climatic forces. Still, we are aware of limitations of this approach: local land use changes or small-scale disturbances in local topography might have triggered additional breakpoints in our area that were not related to climate variability and may also have affected the vegetation's ability to recover after a drought. However, such small-scale disturbances could not have been captured adequately with our 30-m Landsat scale. Besides, no reliable spatially explicit data on the past occurrence of such small-scale disturbances exists. We therefore did not include effects of small-scale disturbances in our study and treated such effects as outliers, for we believed they would not significantly affect the overall distribution of breakpoints within our study area. For example, between 2003 and 2009 we observed a local land use change in the northeast of

our study area (based on Quickbird imagery), appearing like the opening of a soil dumping site. Yet, this local land use change affected only 2% of more than 3000 pixels that were included in our analysis and can therefore be treated as an outlier. Using a more detailed spatial scale would probably increase the effects of small-scale disturbances on the spatial occurrence of breakpoints.

Other factors might also have affected the overall number of breakpoints. Watts and Laffan (2014) found that the optimal value for the "h" parameter, which sets the minimum number of observations between two breakpoints in the BFAST model, depends on vegetation type. In areas with little vegetation cover, the number of breakpoints might be overestimated. Our results, however, revealed an overrepresentation of pixels with none or one breakpoint in areas with low NDVI, and therefore appear to be robust even with this limitation. The same holds true for potentially noise-induced breakpoints, which might have occurred in areas with low NDVI that have a low signal to noise ratio. Data availability is another relevant factor affecting the likelihood to detect breakpoints with BFAST. Temporal satellite data availability was not constant (Figure 5F). Low data availability in 1990 might be a reason why we observed few breakpoints during the dry period 1990/91, compared to the dry period 2005-08. However, since temporal data availability relates to our complete study area, it does not affect the spatial distribution of breakpoints. In contrast, spatial data availability in our study area was not uniform, since clouds were masked on a pixel by pixel level. Hence, cloud-masking on pixel level, could have affected our results.

By using the linear NDVI recovery trend fitted by the BFAST model after a breakpoint as an indicator for the recovery rate, we assumed a linear recovery behaviour. We are aware that this assumption is a simplification, yet we believe it to be a good approximation, as long as the time period of the segment for which the recovery trend is fitted is comparable among pixels. In our case this requirement is fulfilled, since the NDVI recovery trend is fitted to the last segment of the BFAST time series and almost none of the pixels experienced a second breakpoint before the end of the time series (Figure 5D).

We measured grazing intensity indirectly through interviews with local farmers, which were input for calculations based on the distance to the farm, number of animals in farm and topography. Actual data about the grazing intensity (e.g. through GPS tracking) was not available for our time period. In general, it is very difficult to obtain the actual time, location and length of grazing, which can differ even for pastures with the same grazing season (e.g. summer or winter) (Wang et al., 2018). Therefore, the number of animals and the distance to the farm is commonly used as a proxy for grazing intensity (Manthey and Peper, 2010; Wang et al., 2018). To draw more general conclusions on grazing effects on resistance and recovery, future studies applying a consistent methodology on different ecosystems and comparing different spatial scales are needed.

5. Conclusion and Outlook

This study demonstrates the potential of a Landsat NDVI time series to infer two aspects of ecological resilience (namely resistance to climate variability and recovery from drought) of a grazed dryland ecosystem using a change detection method (BFAST). The overall aim of this paper was to spatially quantify resistance and recovery on an ecological meaningful scale and to assess how these two aspects of resilience were modulated by grazing intensity and environmental properties. Our results show that favourable environmental conditions (high NDVI and northern orientation) were related to high resilience, i.e. high resistance to climate variability and fast recovery after a drought. Unfavourable conditions as well as high grazing intensities were related to an unresponsive, potentially degraded ecosystem state. Grazing reduced recovery rate after drought. Overall, we conclude that resilience to climatic variation such as droughts was modulated by grazing and environmental conditions.

Our study presents a new methodology to estimate two aspects of resilience in a natural system on the basis of stochastic natural climatic variation (as has been suggested e.g. by van Nes and Scheffer, 2007), as opposed to using experimental perturbations, which are difficult to apply in coherent natural systems. Quantifying and combining both resistance and recovery in context with grazing data is a novel approach. By applying an adapted version of the BFAST algorithm that can deal with missing

data, we were able to make use of all available Landsat data, enabling us to cover 28 years of vegetation dynamics on an ecological meaningful spatial scale. While several previous studies have made use of a BFAST model to make inferences on vegetation recovery after a disturbance (e.g. DeVries et al., 2015; Katagis et al., 2014; Zewdie et al., 2017), it is a novel approach to make use of the spatial distribution of the number breakpoints to explicitly gain insights on vegetation resistance. We believe our data-driven approach has a strong potential for resilience monitoring, since it can be applied on broad spatial as well as temporal scales and is applicable to areas with a low field data availability. It allows to jointly extract indicators for resistance and recovery, which are two important components of resilience. However, more research on other study areas is needed to test the robustness of our approach.

Extensive research based on mathematical models has focused on resilience in the context of predicting abrupt system transitions (e.g. Kéfi et al., 2014; Scheffer et al., 2015). However, these studies mainly focus on theoretical relationships without fully incorporating the local ecological mechanisms - a solid understanding of which is required for any actions to prevent such transitions (Maestre et al., 2016). In this study we illustrated how two aspects of resilience derived from satellite time series can be related to terrain, NDVI and local knowledge on grazing. Knowledge of how terrain and NDVI affect the vegetation's resilience to climatic variation such as droughts can highlight areas which are particularly susceptible to climate-triggered land degradation processes. An understanding of how different grazing intensities modulate vegetation resilience can enable land users to adapt their grazing management accordingly. However, the results presented here are limited to our study area in southern Cyprus. To draw more general conclusions, further testing of the methodological framework in comparable Mediterranean rangelands is be needed. Also, including other satellite derived vegetation indices such as the Enhanced Vegetation Index (EVI) or the Soil Adjusted Vegetation Index (SAVI), could show if the results on breakpoint occurrence and NDVI recovery trend are sensitive to the chosen vegetation index particularly in sparsely vegetated areas. It would also be interesting to combine our approach with data on plant productivity and soil fertility (see e.g. Berdugo et al., 2020).

Finally, field-based observations of resistance to climate variability and recovery from drought under different grazing pressures would be a valuable addition to our framework to draw comprehensive conclusions on ecosystem resilience.

6. Author Contributions Statement

J.v.K and M.d.H. contributed to the design of the research, wrote the paper in equal parts and performed the analysis of the results. J.v.K performed the pre-processing of the satellite data, implemented the change detection algorithm and did the analysis of the number of breakpoints in relation to grazing and environmental factors. M.d.H. conducted interviews about the grazing history, generated the grazing intensity index and performed the analysis of the factors affecting the NDVI recovery trend. S. F. gave guidance in the design and implementation of the research, particularly the analysis of the satellite data. A.G.M, S.C.D and M.R. contributed to the design of the concepts and objectives in the paper. All authors discussed the results and commented on the manuscript.

7. Funding

This work was supported by the Deutsche Forschungsgemeinschaft (DFG) within the research training group NatRiskChange [grant number GRK 2043/1]; and by NWO and SENSE Research School within the Graduate Programme “Complex Dynamics in Human-Environment Systems” [project number 022.003.009].

8. Acknowledgements

We would like to thank Ben de Vries, Jan Verbesselt and Achim Zeileis for their valuable advice on the implementation of the BFAST algorithm for an irregular Landsat time series. We would also like to thank Daniel Scheffler for his assistance with the geometric co-registration with AROSIC, Lars Schulz for his assistance in implementing the atmospheric correction with the LEDAPS algorithm and Ugur Öztürk for his advice on the Kernel density estimations. Gerald Dörflinger assisted in the acquisition of

the meteorological data, which we highly appreciate. We are grateful to the farmers in the Randi Forest for providing the information about animal stocking numbers. We want to acknowledge the technical support on computation provided by Sylvia Magnussen (GFZ) and thank NASA and ESA for providing the Landsat data used in this study. Finally, we thank the anonymous reviewers for their constructive comments, which considerably helped to improve this manuscript.

9. Literature

Bai, J., Perron, P., 1998. Estimating and Testing Linear Models with Multiple Structural Changes. Econometrica 66, 47. https://doi.org/10.2307/2998540

Ben Abbes, A., Bounouh, O., Farah, I.R., de Jong, R., Martínez, B., 2018. Comparative study of three satellite image time-series decomposition methods for vegetation change detection. European Journal of Remote Sensing 51, 607–615. https://doi.org/10.1080/22797254.2018.1465360

Berdugo, M., Delgado-Baquerizo, M., Soliveres, S., Hernández-Clemente, R., Zhao, Y., Gaitán, J.J., Gross, N., Saiz, H., Maire, V., Lehman, A., Rillig, M.C., Solé, R.V., Maestre, F.T., 2020. Global ecosystem thresholds driven by aridity. Science 367, 787–790. https://doi.org/10.1126/science.aay5958

Bernardino, P.N., Keersmaecker, W.D., Fensholt, R., Verbesselt, J., Somers, B., Horion, S., 2020. Global-scale characterization of turning points in arid and semi-arid ecosystem functioning. Global Ecology and Biogeography 29, 1230–1245. https://doi.org/10.1111/geb.13099

Browning, D.M., Maynard, J.J., Karl, J.W., Peters, D.C., 2017. Breaks in MODIS time series portend vegetation change: verification using long-term data in an arid grassland ecosystem. Ecological Applications 27, 1677–1693. https://doi.org/10.1002/eap.1561

Dakos, V., Carpenter, S.R., van Nes, E.H., Scheffer, M., 2014. Resilience indicators: prospects and limitations for early warnings of regime shifts. Philosophical Transactions of the Royal Society B: Biological Sciences 370, 20130263–20130263. https://doi.org/10.1098/rstb.2013.0263

Daliakopoulos, I., Tsanis, I., 2014. Historical evolution of dryland ecosystems. CASCADE Project Deliverable 2.1. CASCADE Report 04. www.cascadis-project.eu/documents (accessed 31 January 2019).

de Jong, R., Verbesselt, J., Zeileis, A., Schaepman, M., 2013. Shifts in Global Vegetation Activity Trends. Remote Sensing 5, 1117–1133. https://doi.org/10.3390/rs5031117

De Keersmaecker, W., Lhermitte, S., Tits, L., Honnay, O., Somers, B., Coppin, P., 2015. A model quantifying global vegetation resistance and resilience to short-term climate anomalies and their relationship with vegetation cover: Global vegetation resistance and resilience. Global Ecology and Biogeography 24, 539–548. https://doi.org/10.1111/geb.12279

De Keersmaecker, W., van Rooijen, N., Lhermitte, S., Tits, L., Schaminee, J., Coppin, P., Honnay, O., Somers, B., 2016. Species-rich semi-natural grasslands have a higher resistance but a lower resilience than intensively managed agricultural grasslands in response to climate anomalies. Journal of Applied Ecology 53, 430–439. https://doi.org/10.1111/1365-2664.12595

del Barrio, G., Puigdefabregas, J., Sanjuan, M.E., Stellmes, M., Ruiz, A., 2010. Assessment and monitoring of land condition in the Iberian Peninsula, 1989–2000. Remote Sensing of Environment 114, 1817–1832. https://doi.org/10.1016/j.rse.2010.03.009

DeVries, B., Decuyper, M., Verbesselt, J., Zeileis, A., Herold, M., Joseph, S., 2015a. Tracking disturbance-regrowth dynamics in tropical forests using structural change detection and Landsat time series. Remote Sensing of Environment 169, 320–334. https://doi.org/10.1016/j.rse.2015.08.020

DeVries, B., Pratihast, A.K., Verbesselt, J., Kooistra, L., Herold, M., 2016. Characterizing Forest Change Using Community-Based Monitoring Data and Landsat Time Series. PLOS ONE 11, e0147121. https://doi.org/10.1371/journal.pone.0147121

DeVries, B., Verbesselt, J., Kooistra, L., Herold, M., 2015b. Robust monitoring of small-scale forest disturbances in a tropical montane forest using Landsat time series. Remote Sensing of Environment 161, 107–121. https://doi.org/10.1016/j.rse.2015.02.012

Dougill, A.J., Thomas, D.S.G., Heathwaite, A.L., 1999. Environmental change in the Kalahari: Integrated land degradation studies for nonequilibrium dryland environments. Annals of the Association of American Geographers 89, 420–442. https://doi.org/10.1111/0004-5608.00156

Dutrieux, L.P., Verbesselt, J., Kooistra, L., Herold, M., 2015. Monitoring forest cover loss using multiple data streams, a case study of a tropical dry forest in Bolivia. ISPRS Journal of Photogrammetry and Remote Sensing 107, 112–125. https://doi.org/10.1016/j.isprsjprs.2015.03.015

Frazier, A.E., Renschler, C.S., Miles, S.B., 2013. Evaluating post-disaster ecosystem resilience using MODIS GPP data. International Journal of Applied Earth Observation and Geoinformation 21, 43–52. https://doi.org/10.1016/j.jag.2012.07.019

Gaitán, J.J., Bran, D., Oliva, G., Ciari, G., Nakamatsu, V., Salomone, J., Ferrante, D., Buono, G., Massara, V., Humano, G., Celdrán, D., Opazo, W., Maestre, F.T., 2013. Evaluating the performance of multiple remote sensing indices to predict the spatial variability of ecosystem structure and functioning in Patagonian steppes. Ecological Indicators 34, 181–191. https://doi.org/10.1016/j.ecolind.2013.05.007

Goward, S., Arvidson, T., Williams, D., Faundeen, J., Irons, J., Franks, S., 2006. Historical Record of Landsat Global Coverage. Photogrammetric Engineering & Remote Sensing 72, 1155–1169. https://doi.org/10.14358/PERS.72.10.1155

Hansen, M.C., Loveland, T.R., 2012. A review of large area monitoring of land cover change using Landsat data. Remote Sensing of Environment 122, 66–74. https://doi.org/10.1016/j.rse.2011.08.024

Helman, D., Mussery, A., Lensky, I.M., Leu, S., 2014. Detecting changes in biomass productivity in a different land management regimes in drylands using satellite-derived vegetation index. Soil Use and Management 30, 32–39. https://doi.org/10.1111/sum.12099

Henebry, G.M., 2019. Methodology II: Remote sensing of change in grasslands, in: Gibson, D.J., Newman, J.A. (Eds.), Grasslands and Climate Change. Cambridge University Press, pp. 40–64. https://doi.org/10.1017/9781108163941.005

Hodgson, D., McDonald, J.L., Hosken, D.J., 2015. What do you mean, 'resilient'? Trends in Ecology & Evolution 30, 503–506. https://doi.org/10.1016/j.tree.2015.06.010

Holling, C.S., 1996. Engineering Resilience versus Ecological Resilience, in: Schulze, P.C. (Ed.), Engineering Within Ecological Constraints. The National Academies Press, Washington, DC, pp. 31–43.

Holling, C.S., 1973. Resilience and Stability of Ecological Systems. Annual Review of Ecology and Systematics 4, 1–23. https://doi.org/10.1146/annurev.es.04.110173.000245

Huang, K., Zhou, T., Zhao, X., 2014. Extreme Drought-induced Trend Changes in MODIS EVI Time Series in Yunnan, China. IOP Conference Series: Earth and Environmental Science 17, 012070. https://doi.org/10.1088/1755-1315/17/1/012070

Ingrisch, J., Bahn, M., 2018. Towards a Comparable Quantification of Resilience. Trends in Ecology & Evolution 33, 251–259. https://doi.org/10.1016/j.tree.2018.01.013

IPCC, 2014. Climate Change 2014: Impacts, Adaptation, and Vulnerability. Part B: Regional Aspects. Contribution of Working Group II to the Fifth Assessment Report of the Intergovernmental Panel on Climate Change. Cambridge University Press, Cambridge, United Kingdom and New York, NY, USA.

IUSS Working Group WRB, 2015. World Reference Base for Soil Resources 2014, update 2015 International soil classification system for naming soils and creating legends for soil maps. World Soil Resources Reports No. 106, FAO, Rome. http://www.fao.org/3/i3794en/I3794en.pdf (accessed 12 November 2018).

Katagis, T., Gitas, I.Z., Toukiloglou, P., Veraverbeke, S., Goossens, R., 2014. Trend analysis of medium- and coarse-resolution time series image data for burned area mapping in a Mediterranean ecosystem. Int. J. Wildland Fire 23, 668–677. https://doi.org/10.1071/WF12055

Kawamura, K., Akiyama, T., Yokota, H., Tsutsumi, M., Yasuda, T., Watanabe, O., Wang, S., 2005. Quantifying grazing intensities using geographic information systems and satellite remote sensing in the Xilingol steppe region, Inner Mongolia, China. Agriculture, Ecosystems & Environment 107, 83–93. https://doi.org/10.1016/j.agee.2004.09.008

Kéfi, S., Guttal, V., Brock, W.A., Carpenter, S.R., Ellison, A.M., Livina, V.N., Seekell, D.A., Scheffer, M., van Nes, E.H., Dakos, V., 2014. Early Warning Signals of Ecological Transitions: Methods for Spatial Patterns. PLOS ONE 9, e92097. https://doi.org/10.1371/journal.pone.0092097

Kennedy, R.E., Andréfouët, S., Cohen, W.B., Gómez, C., Griffiths, P., Hais, M., Healey, S.P., Helmer, E.H., Hostert, P., Lyons, M.B., Meigs, G.W., Pflugmacher, D., Phinn, S.R., Powell, S.L., Scarth, P., Sen, S., Schroeder, T.A., Schneider, A., Sonnenschein, R., Vogelmann, J.E., Wulder, M.A., Zhu, Z., 2014. Bringing an ecological view of change to Landsat-based remote sensing. Frontiers in Ecology and the Environment 12, 339–346. https://doi.org/10.1890/130066

Kovalskyy, V., Roy, D.P., 2013. The global availability of Landsat 5 TM and Landsat 7 ETM+ land surface observations and implications for global 30m Landsat data product generation. Remote Sensing of Environment 14.

Lambert, J., Drenou, C., Denux, J.-P., Balent, G., Cheret, V., 2013. Monitoring forest decline through remote sensing time series analysis. GIScience & Remote Sensing 50, 437–457. https://doi.org/10.1080/15481603.2013.820070

López, D.R., Brizuela, M.A., Willems, P., Aguiar, M.R., Siffredi, G., Bran, D., 2013. Linking ecosystem resistance, resilience, and stability in steppes of North Patagonia. Ecological Indicators 24, 1–11. https://doi.org/10.1016/j.ecolind.2012.05.014

Maestre, F.T., Eldridge, D.J., Soliveres, S., Kéfi, S., Delgado-Baquerizo, M., Bowker, M.A., García-Palacios, P., Gaitán, J., Gallardo, A., Lázaro, R., Berdugo, M., 2016. Structure and Functioning of Dryland Ecosystems in a Changing World. Annual Review of Ecology, Evolution, and Systematics 47, 215–237. https://doi.org/10.1146/annurev-ecolsys-121415-032311

Manthey, M., Peper, J., 2010. Estimation of grazing intensity along grazing gradients – the bias of nonlinearity. Journal of Arid Environments 74, 1351–1354. https://doi.org/10.1016/j.jaridenv.2010.05.007

Masek, J.G., Vermote, E.F., Saleous, N.E., Wolfe, R., Hall, F.G., Huemmrich, K.F., Gao, F., Kutler, J., Lim, T.-K., 2006. A Landsat Surface Reflectance Dataset for North America, 1990–2000. IEEE Geoscience and Remote Sensing Letters 3, 68–72. https://doi.org/10.1109/LGRS.2005.857030

Mayor, Á.G., Kéfi, S., Bautista, S., Rodríguez, F., Cartení, F., Rietkerk, M., 2013. Feedbacks between vegetation pattern and resource loss dramatically decrease ecosystem resilience and restoration potential in a simple dryland model. Landscape Ecology 28, 931–942. https://doi.org/10.1007/s10980-013-9870-4

Nimmo, D.G., Mac Nally, R., Cunningham, S.C., Haslem, A., Bennett, A.F., 2015. Vive la résistance: reviving resistance for 21st century conservation. Trends in Ecology & Evolution 30, 516–523. https://doi.org/10.1016/j.tree.2015.07.008

Noy-Meir, I., 1975. Stability of Grazing Systems: An Application of Predator-Prey Graphs. Journal of Ecology 63, 459–481. https://doi.org/10.2307/2258730

Peterson, G., Allen, C.R., Holling, C.S., 1998. Ecological resilience, biodiversity, and scale. Ecosystems 1, 6–18. https://doi.org/10.1007/s100219900002

Pettorelli, N., Vik, J.O., Mysterud, A., Gaillard, J.-M., Tucker, C.J., Stenseth, N.C., 2005. Using the satellite-derived NDVI to assess ecological responses to environmental change. Trends in Ecology & Evolution 20, 503–510. https://doi.org/10.1016/j.tree.2005.05.011

Pinheiro, J., Bates, D., DebRoy, S., Sarkar, D., 2018. Nlme: Linear and Nonlinear Mixed Effects Models. R package version 3.1-137. https://CRAN.R-project.org/package=nlme.

Platt, R.V., Ogra, M.V., Badola, R., Hussain, S.A., 2016. Conservation-induced resettlement as a driver of land cover change in India: An object-based trend analysis. Applied Geography 69, 75–86. https://doi.org/10.1016/j.apgeog.2016.02.006

R Core Team, 2017. A language and environment for statistical computing. R Foundation for Statistical Computing, Vienna, Austria. http://www.R-project.org/.

Republic of Cyprus: Meteorological Service, 2019. Climate of Cyprus. http://www.moa.gov.cy/moa/ms/ms.nsf/DMLcyclimate_en/DMLcyclimate_en?OpenDocument (accessed 22 August 2019).

Ruppert, J.C., Harmoney, K., Henkin, Z., Snyman, H.A., Sternberg, M., Willms, W., Linstaedter, A., 2015. Quantifying drylands' drought resistance and recovery: the importance of drought intensity, dominant life history and grazing regime. Global Change Biology 21, 1258–1270. https://doi.org/10.1111/gcb.12777

Saruul, K., Jiangwen, L., Jianming, N., Qing, Z., Xuefeng, Z., Guodong, H., Mengli, Z., Haifeng, B., 2019. Typical steppe ecosystems maintain high stability by decreasing the connections among recovery, resistance, and variability under high grazing pressure. Science of The Total Environment 659, 1146–1157. https://doi.org/10.1016/j.scitotenv.2018.12.447

Scheffer, M., Carpenter, S., Foley, J.A., Folke, C., Walker, B., 2001. Catastrophic shifts in ecosystems. Nature 413, 591–596. https://doi.org/10.1038/35098000

Scheffer, M., Carpenter, S.R., Dakos, V., van Nes, E.H., 2015. Generic Indicators of Ecological Resilience: Inferring the Chance of a Critical Transition. Annual Review of Ecology, Evolution, and Systematics 46, 145–167. https://doi.org/10.1146/annurev-ecolsys-112414-054242

Scheffer, M., Carpenter, S.R., Lenton, T.M., Bascompte, J., Brock, W., Dakos, V., van de Koppel, J., van de Leemput, I.A., Levin, S.A., van Nes, E.H., Pascual, M., Vandermeer, J., 2012. Anticipating Critical Transitions. Science 338, 344–348. https://doi.org/10.1126/science.1225244

Scheffler, D., Hollstein, A., Diedrich, H., Segl, K., Hostert, P., 2017. AROSICS: An Automated and Robust Open-Source Image Co-Registration Software for Multi-Sensor Satellite Data. Remote Sensing 9, 676. https://doi.org/10.3390/rs9070676

Schmidt, G., Jenkerson, C.B., Masek, J., Vermote, E., Gao, F., 2013. Landsat ecosystem disturbance adaptive processing system (LEDAPS) algorithm description (Report No. 2013–1057), Open-File Report. Reston, VA. https://doi.org/10.3133/ofr20131057

Schneider, F.D., Kéfi, S., 2016. Spatially heterogeneous pressure raises risk of catastrophic shifts. Theoretical Ecology 9, 207–217. https://doi.org/10.1007/s12080-015-0289-1

Schwalm, C.R., Anderegg, W.R.L., Michalak, A.M., Fisher, J.B., Biondi, F., Koch, G., Litvak, M., Ogle, K., Shaw, J.D., Wolf, A., Huntzinger, D.N., Schaefer, K., Cook, R., Wei, Y., Fang, Y., Hayes, D., Huang, M., Jain, A., Tian, H., 2017. Global patterns of drought recovery. Nature 548, 202–205. https://doi.org/10.1038/nature23021

Simoniello, T., Lanfredi, M., Liberti, M., Coppola, R., Macchiato, M., 2008. Estimation of vegetation cover resilience from satellite time series. Hydrology and Earth System Sciences 12, 1053–1064. https://doi.org/10.5194/hess-12-1053-2008

van de Leemput, I.A., Dakos, V., Scheffer, M., van Nes, E.H., 2018. Slow Recovery from Local Disturbances as an Indicator for Loss of Ecosystem Resilience. Ecosystems 21, 141–152. https://doi.org/10.1007/s10021-017-0154-8

van Nes, E.H., Scheffer, M., 2007. Slow Recovery from Perturbations as a Generic Indicator of a Nearby Catastrophic Shift. The American Naturalist 169, 738–747. https://doi.org/10.1086/516845

Verbesselt, J., Hyndman, R., Newnham, G., Culvenor, D., 2010a. Detecting trend and seasonal changes in satellite image time series. Remote Sensing of Environment 114, 106–115. https://doi.org/10.1016/j.rse.2009.08.014

Verbesselt, J., Hyndman, R., Zeileis, A., Culvenor, D., 2010b. Phenological change detection while accounting for abrupt and gradual trends in satellite image time series. Remote Sensing of Environment 114, 2970–2980. https://doi.org/10.1016/j.rse.2010.08.003

Verbesselt, J., Zeileis, A., Herold, M., 2012. Near real-time disturbance detection using satellite image time series. Remote Sensing of Environment 123, 98–108. https://doi.org/10.1016/j.rse.2012.02.022

Vicente-Serrano, S.M., Gouveia, C., Camarero, J.J., Begueria, S., Trigo, R., Lopez-Moreno, J.I., Azorin-Molina, C., Pasho, E., Lorenzo-Lacruz, J., Revuelto, J., Moran-Tejeda, E., Sanchez-Lorenzo, A., 2013. Response of vegetation to drought time-scales across global land biomes. Proceedings of the National Academy of Sciences 110, 52–57. https://doi.org/10.1073/pnas.1207068110

Wang, Y., Lehnert, L.W., Holzapfel, M., Schultz, R., Heberling, G., Görzen, E., Meyer, H., Seeber, E., Pinkert, S., Ritz, M., Fu, Y., Ansorge, H., Bendix, J., Seifert, B., Miehe, G., Long, R.-J., Yang, Y.-P., Wesche, K., 2018. Multiple indicators yield diverging results on grazing degradation and

climate controls across Tibetan pastures. Ecological Indicators 93, 1199–1208. https://doi.org/10.1016/j.ecolind.2018.06.021

Washington-Allen, R., Ramsey, R., West, N., Norton, B., 2008. Quantification of the ecological resilience of drylands using digital remote sensing. Ecology and Society 13. https://doi.org/10.5751/ES-02489-130133

Watts, L.M., Laffan, S.W., 2014. Effectiveness of the BFAST algorithm for detecting vegetation response patterns in a semi-arid region. Remote Sensing of Environment 154, 234–245. https://doi.org/10.1016/j.rse.2014.08.023

Watts, L.M., Laffan, S.W., 2013. Sensitivity of the BFAST algorithm to MODIS satellite and vegetation index. Modelling & Simulation Soc Australia & New Zealand Inc, Christchurch.

Weiss, J.L., Gutzler, D.S., Coonrod, J.E.A., Dahm, C.N., 2004. Long-term vegetation monitoring with NDVI in a diverse semi-arid setting, central New Mexico, USA. Journal of Arid Environments 58, 249–272. https://doi.org/10.1016/j.jaridenv.2003.07.001

Whitford, W.G., Rapport, D.J., deSoyza, A.G., 1999. Using resistance and resilience measurements for "fitness" tests in ecosystem health. J. Environ. Manage. 57, 21–29. https://doi.org/10.1006/jema.1999.0287

Zeileis, A., Kleiber, C., Krämer, W., Hornik, K., 2003. Testing and dating of structural changes in practice. Computational Statistics & Data Analysis 44, 109–123. https://doi.org/10.1016/S0167-9473(03)00030-6

Zeileis, A., Leisch, F., Hornik, K., Kleiber, C., 2002. strucchange. An R package for testing for structural change in linear regression models. Journal of Statistical Software 7, 1–38. https://doi.org/10.18637/jss.v007.i02

Zewdie, W., Csaplovics, E., Inostroza, L., 2017. Monitoring ecosystem dynamics in northwestern Ethiopia using NDVI and climate variables to assess long term trends in dryland vegetation variability. Applied Geography 79, 167–178. https://doi.org/10.1016/j.apgeog.2016.12.019

Zhou, Z.C., Gan, Z.T., Shangguan, Z.P., Dong, Z.B., 2010. Effects of grazing on soil physical properties and soil erodibility in semiarid grassland of the Northern Loess Plateau (China). CATENA 82, 87–91. https://doi.org/10.1016/j.catena.2010.05.005

Zhu, Z., Woodcock, C.E., 2014. Continuous change detection and classification of land cover using all available Landsat data. Remote Sensing of Environment 144, 152–171. https://doi.org/10.1016/j.rse.2014.01.011

Supplementary material

Supplementary material of the manuscript “Resilience of vegetation to drought: studying the effect of grazing in a Mediterranean rangeland using satellite time series” by J. von Keyserlingk, M. de Hoop, A.G. Mayor, S.C. Dekker, M. Rietkerk, S. Foerster

S1. Monthly rainfall and precipitation

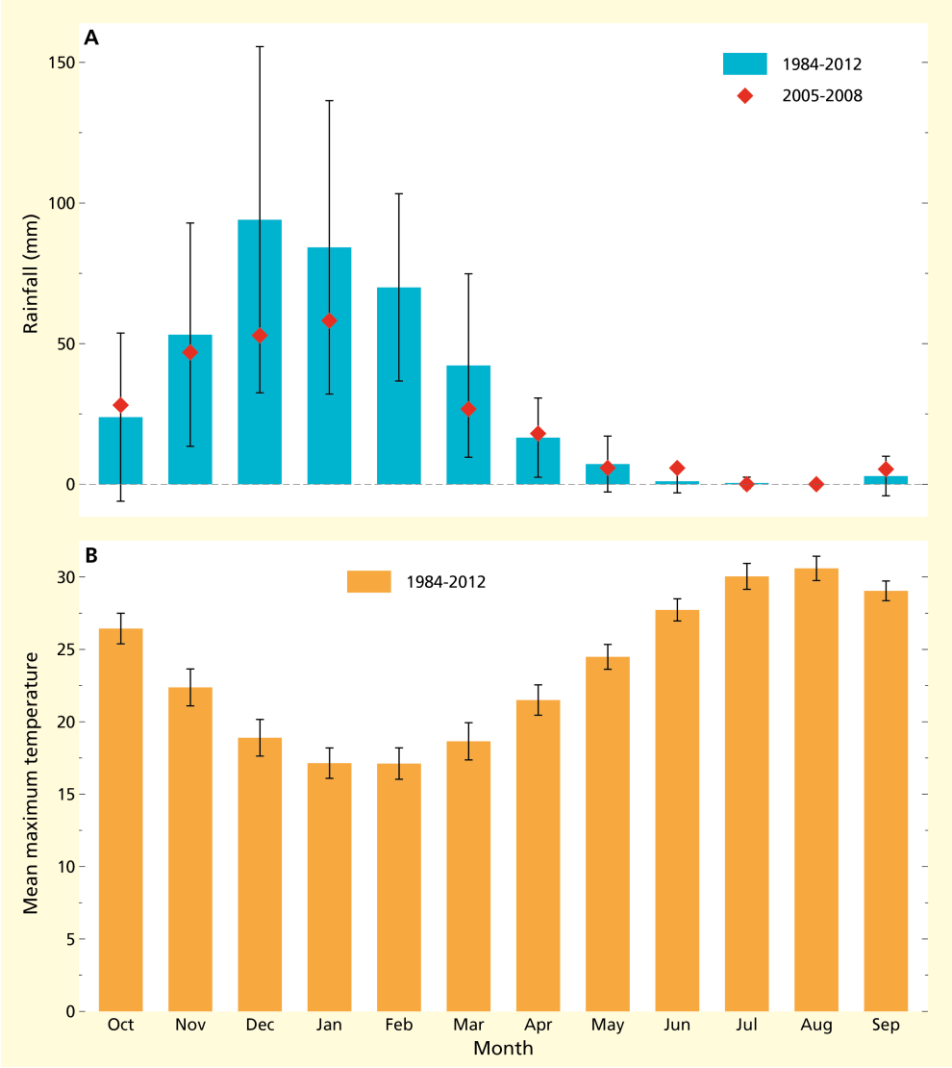

Figure S1. Monthly mean rainfall (A) and maximum temperature (B) for the hydrological years 1984-2012. Error bars show the standard deviation (±1SD). The red triangles in A represent the mean monthly rainfall for the hydrological years 2005-2008. This time period represents the period of drought, which was used for the detection of drought breakpoints. Monthly mean temperature was calculated based on daily maximum temperature measured at meteorological station at Pafos airport. Monthly mean rainfall was calculated based on total daily rainfall measured at meteorological station at Pissouri. All data was obtained from the Meteorological Service of Cyprus.

S2. Satellite Data Pre-processing

Coregistration with AROSICS: As geospatial reference for the co-registration, a cloud-free scene (LE71760362002225SGS00, surface reflectance, band 4), downloaded from USGS archive was used. A scene from the USGS archive was chosen, because the Landsat surface reflectance products are well geospatially aligned among each other, and we wanted to keep the option for including imagery downloaded from USGS in our data analysis later.

Number of valid observations after cloud-masking: s, cloud shadows, snow and missing data were masked on pixel level. Hence, spatial data availability of valid observations varied slightly within our study area.

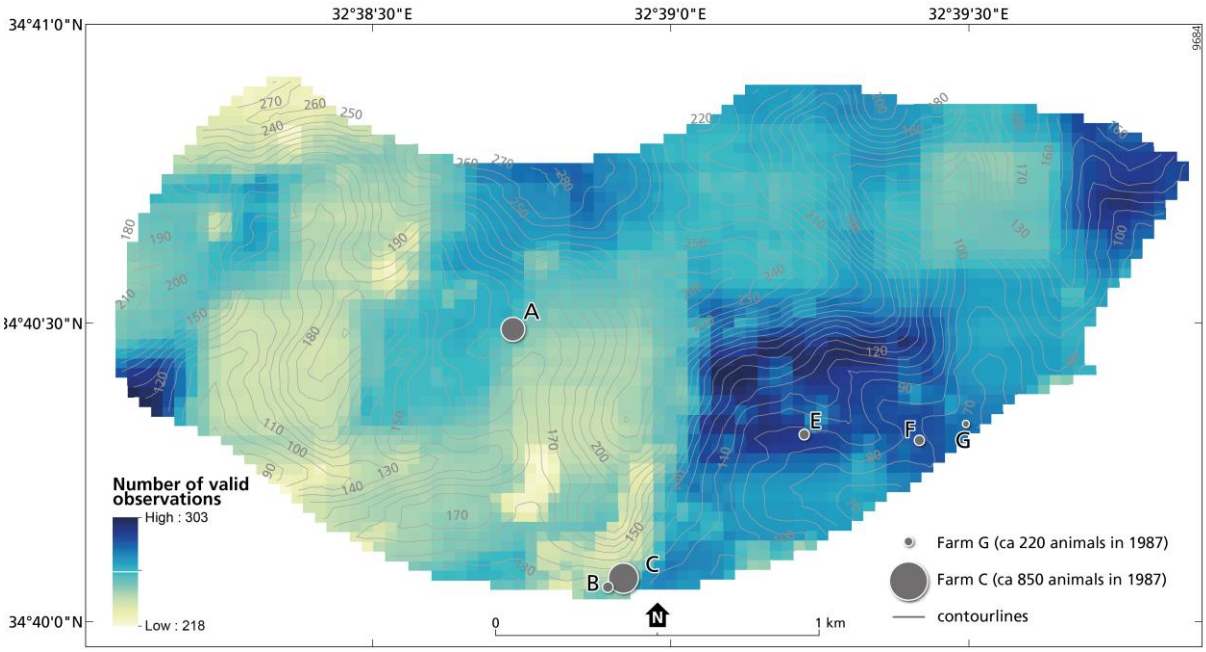

Figure S2. Number of valid observations in our study area during the hydrological years 1984-2012. Valid observations refers to all Landsat pixels free of clouds or cloud shadows that were included in our analysis.

S3. Temporal distribution of Landsat scenes included in the analysis

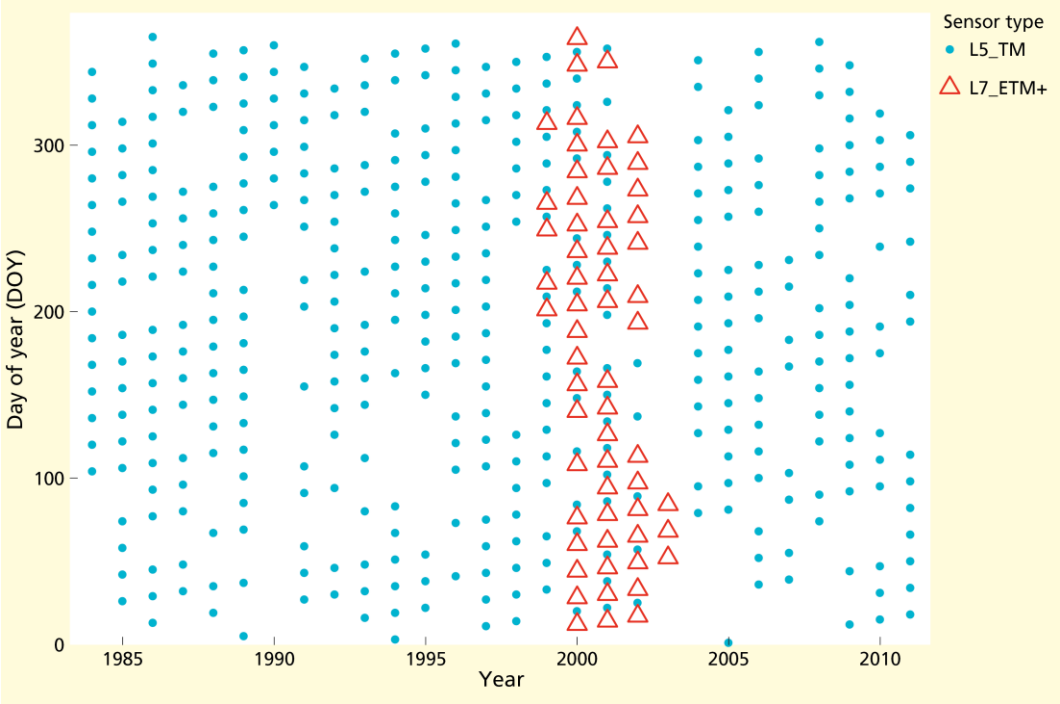

Figure S3. Temporal distribution of all Landsat 5 TM-scenes and Landsat 7 ETM+-scenes that were included in the analysis. Landsat 7 ETM+-scenes affected by the failure of the scan line corrector in 2003 (Landsat 7 ETMP+ SLC-off) were excluded prior to the analysis and are not included in this figure.

S4. Grazing intensity maps

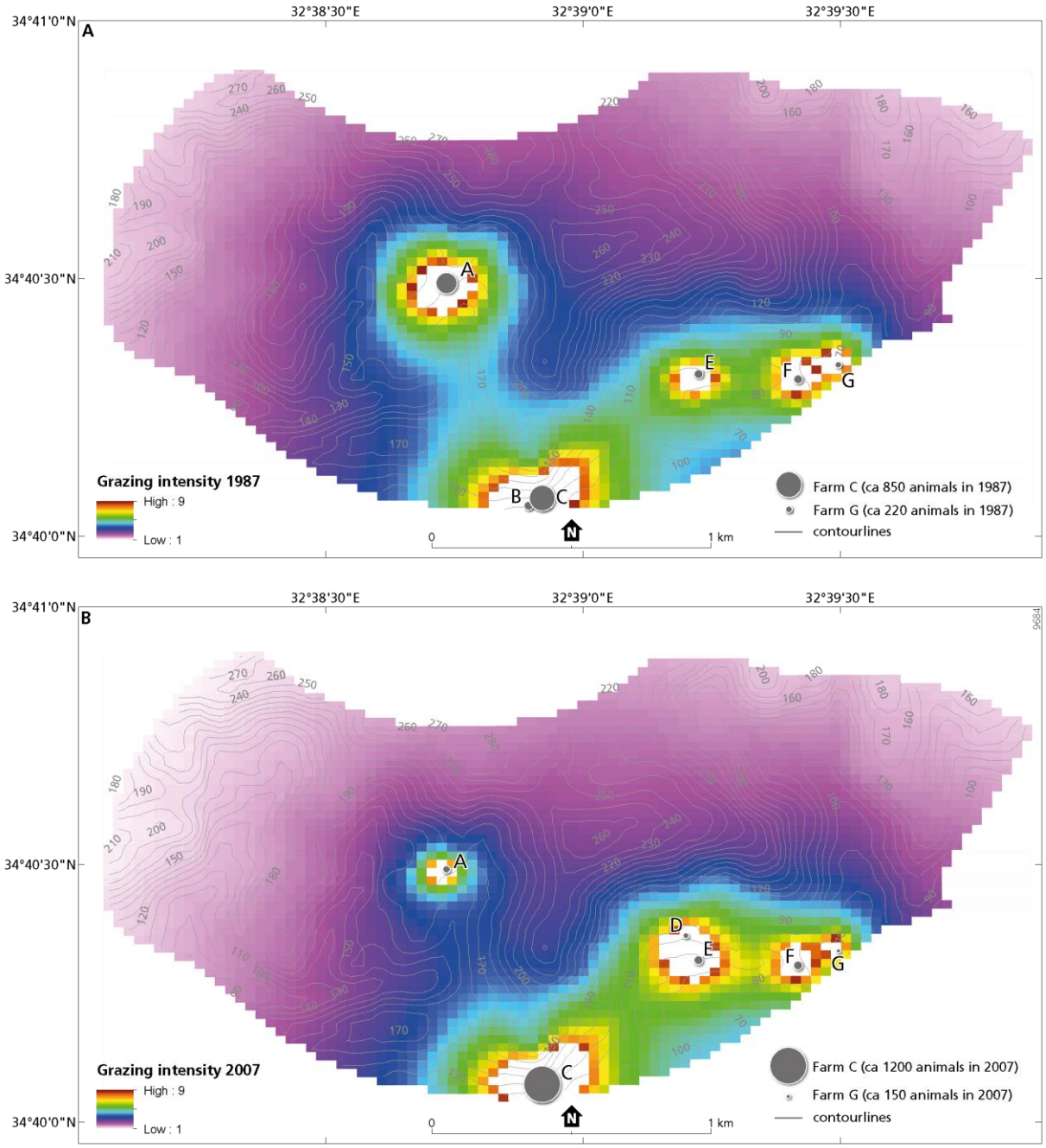

Figure S4. Estimated grazing intensity for 1987 and 2007, based on the number of animals per farm, the inversed distance to the farm and the vertical friction factor (to account for the difficulty to walk up- or downslope). Grazing values above the 97.5% quantile are excluded. Circles depict goat farms with the size of the circle proportional to the estimated number of animals in the specific period.

S5. Detailed results of Kolmogorov-Smirnov test for the analysis of resistance

Table S5. Results from a two-sample Kolmogorov-Smirnov test performed with the R package "stats" (R Core Team, 2017). Significant p values at α = 0.01 are highlighted in grey. The spatial probability distributions of each breakpoint category were calculated and compared to the overall spatial distributions of grazing intensity 1987, mean NDVI, terrain slope and deviation from south in our study area. A significant p value indicates that the two distributions do not share the same underlying continuous distribution. D is calculated as the maximum vertical difference between the cumulative distribution functions of the two samples. Since the breakpoint categories are sub-samples of the overall distributions there are ties present in the data. Hence the p values are an approximation. To account for this issue and to make our results robust, we used a conservative significance level of α = 0.01.

Breakpoint	**Grazing intensity 1987**		**Mean NDVI 1984-2011**		**Terrain slope**		**Deviation from south**	
category	**D (max Δ)**	**p value**	**D (max Δ)**	**p value**	**D (max Δ)**	**p value**	**D (max Δ)**	**p value**
0	0.3	<0.001	0.348	<0.001	0.095	0.049	0.104	0.024
1	0.058	0.013	0.116	<0.001	0.052	0.028	0.059	0.009
2	0.046	0.03	0.037	0.133	0.019	0.847	0.045	0.036
3	0.087	0.001	0.116	<0.001	0.035	0.539	0.077	0.003
4	0.151	0.004	0.135	0.012	0.08	0.34	0.125	0.026

S6. Regression analysis for the NDVI recovery trend

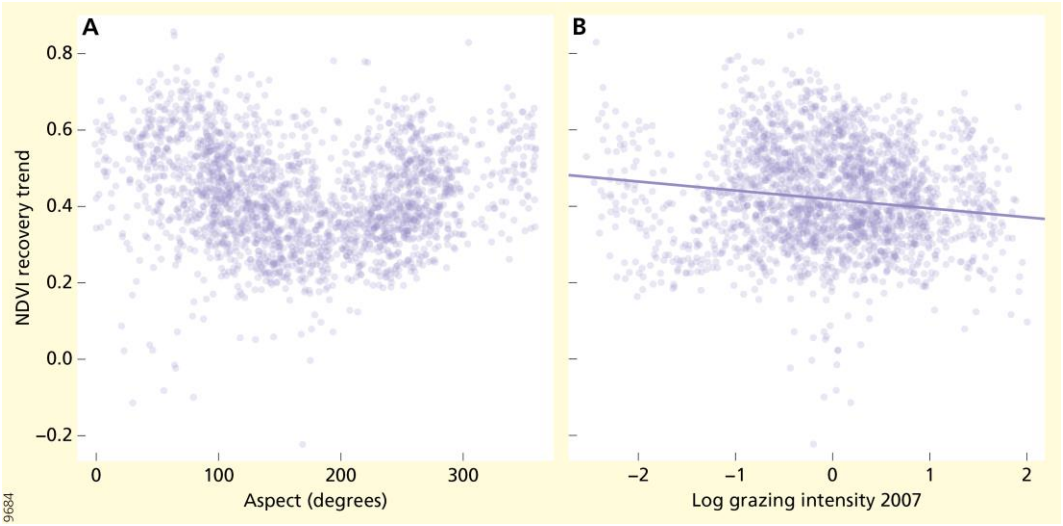

Figure S6. Simple regression analysis between the NDVI recovery trend ($\frac{\Delta NDVI}{day} \times 10{,}000$) after the drought breakpoint and A) aspect B) estimated grazing intensity in 2007 (β=-0.149 p=0.042).